

Boosting Vision-Language Models with Transduction

Maxime Zanella*
UCLouvain

Benoît Gérin*
UCLouvain

Ismail Ben Ayed
ÉTS Montréal

Code: <https://github.com/MaxZanella/transduction-for-vlms>

Abstract

Transduction is a powerful paradigm that leverages the structure of unlabeled data to boost predictive accuracy. We present TransCLIP, a novel and computationally efficient transductive approach designed for Vision-Language Models (VLMs). TransCLIP is applicable as a plug-and-play module on top of popular inductive zero- and few-shot models, consistently improving their performances. Our new objective function can be viewed as a regularized maximum-likelihood estimation, constrained by a KL divergence penalty that integrates the text-encoder knowledge and guides the transductive learning process. We further derive an iterative Block Majorize-Minimize (BMM) procedure for optimizing our objective, with guaranteed convergence and decoupled sample-assignment updates, yielding computationally efficient transduction for large-scale datasets. We report comprehensive evaluations, comparisons, and ablation studies that demonstrate: (i) Transduction can greatly enhance the generalization capabilities of inductive pretrained zero- and few-shot VLMs; (ii) TransCLIP substantially outperforms standard transductive few-shot learning methods relying solely on vision features, notably due to the KL-based language constraint.

1 Introduction

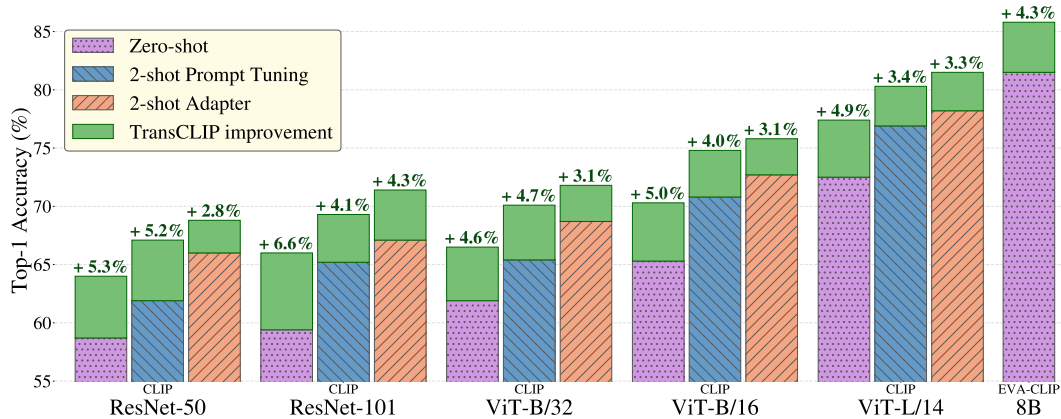


Figure 1: **TransCLIP** improves significantly the averaged top-1 accuracy on 11 datasets when used on top of inductive zero-shot **CLIP**, 2-shot **CoOp** prompt tuning and 2-shot **TaskRes** adapter for various encoder sizes.

*Equal contributions and corresponding authors. {maxime.zanella,benoit.gerin}@uclouvain.be

Combining vision and language modalities can greatly enhance expressiveness and reduce ambiguities in the understanding and interpretation of our environment. This principle is central in the development of Vision-Language Models (VLMs), such as CLIP [49], which learns visual representations through natural-language supervision. In the pre-training phase, an input image \mathbf{x} and associated text description \mathbf{c} are encoded by separate vision and text encoders. This yields feature representations $\mathbf{f} = \theta_v(\mathbf{x})$ and $\mathbf{t} = \theta_t(\mathbf{c})$, which can be aligned by contrastive learning. Such a joint embedding space for the visual and textual modalities facilitates zero-shot recognition and yields powerful adaptation capabilities for a large variety of tasks. The recent literature on adapting VLMs has grown substantially, in both the zero-shot and few-shot learning settings [72, 71, 16, 69, 73, 25, 42]. However, so far, these techniques predominantly align with *induction*, i.e., inference for each test sample is performed independently from the other samples within the target dataset.

In contrast, *transduction* performs joint inference on all the test samples of a task, leveraging the statistics of the target unlabeled data [57, 27, 70]. In the context of standard vision-based classifiers, this has enabled transductive methods to outperform inductive-inference approaches as evidenced by benchmarks over large-scale datasets such as ImageNet [2].

Within the scope of deep learning, transduction has mainly been explored for few-shot learning to address the inherent challenges of training under limited supervision. This recent and quite abundant few-shot literature, e.g., [5, 13, 33, 36, 43, 75, 24, 74], among others, has focused on adopting standard vision-based pre-training models (such as ImageNet pre-training). However, as we will show in our experiments (Table 4), the direct application of existing transductive few-shot methods to VLMs yields poor performances, sometimes underperforming the inductive zero-shot predictions. This might explain why the transductive paradigm has been overlooked in zero-shot and few-shot learning for VLMs so far. The low performance of current transductive few-shot methods in the context of VLMs could be explained by the fact that the underlying objective functions do not account for the text knowledge. However, in this new multi-modal paradigm, additional supervision could be leveraged from the textual descriptions of the classes (prompts) [49], e.g., $\mathbf{c}_k = \text{a photo of a [kth class name]}$, along with their corresponding representation $\mathbf{t}_k = \theta_t(\mathbf{c}_k)$ derived from the language encoder. We utilize the interleaved representation of text prompts and images with their cosine² similarity $\mathbf{f}^\top \mathbf{t}_k$, which yields text-based prediction $\hat{\mathbf{y}}_k$, thereby guiding our transductive optimization procedure with text-encoder knowledge. Our method optimizes a new objective function integrating a text-driven penalty. Optimization is carried out efficiently w.r.t the assignment variables associated with the unlabeled samples, which are then used as final predictions.

Adapting VLMs has recently attracted wide attention in the literature, predominantly focusing on inductive methods. Motivated by findings in NLP, which indicate that better prompt strategies could enhance performance [52, 26, 22], substantial efforts were directed towards prompt tuning [34] for VLMs, with CoOp [72] standing out as the pioneering work along this line. Following CoOp, prompt tuning has become the favorite strategy for adapting VLMs in a variety of contexts, including unsupervised [25, 42, 15, 40, 1] and few-shot [72, 71, 39, 12, 64, 6, 73, 8, 9, 29, 30, 66] learning. Meanwhile, there have been a few efforts towards computationally more efficient adapters [69, 47, 65]. Our transduction formulation aligns with this initiative. By operating solely on the output embeddings (i.e., in a black-box setting), TransCLIP is computationally efficient and does not make assumptions on the underlying encoder architectures. Still, our method is orthogonal to these design choices and could be applied atop any of the above-mentioned inductive approaches.

Main contributions. (i) We introduce a transductive formulation that enhances the zero-shot and few-shot generalization capabilities of VLMs by leveraging the structure of unlabeled data (Figure 1). Our new objective function can be viewed as a regularized maximum-likelihood estimation, constrained by a Kullback-Leibler (KL) divergence penalty integrating the text-encoder knowledge and guiding the transductive learning process. We further derive an iterative Block Majorize-Minimize (BMM) procedure for optimizing our objective, with guaranteed convergence and decoupled sample-assignment updates, yielding computationally efficient transduction for large-scale datasets, such as ImageNet. (ii) Our method can be used as a plug-and-play module on top of current inductive zero-shot models and few-shot learning methods, consistently boosting their performance. Also, (iii) our approach substantially outperforms recent transductive few-shot methods in the literature, notably due to the KL-based language supervision as a critical success factor.

²In VLMs, such as CLIP [49], both visual and text embeddings are normalized (i.e., are within the unit hyper-sphere). Thus, the cosine similarity corresponds to the dot product.

2 Related Work

Transduction for vision-only classifiers. The use of unlabeled test data at inference time has received attention lately in rapidly emerging subjects, such as few-shot learning and unsupervised test-time adaptation. Examples include adjusting batch normalization layer statistics [45] and minimizing the entropy of predictions [59], which can be supplemented by pseudo-labeling strategies [35]. In the few-shot literature solely based on vision models, transduction leverages both the few labeled samples and unlabeled test data, outperforming inductive methods [75, 5, 24, 36, 74]. One of the first works introducing transduction in vision-based few-shot learning proposes propagating the labels from the support (labeled) to the query (unlabeled) set with a meta-learned graph [38]. Building on this idea, another work proposes to iteratively augment the support set to improve label propagation [33]. LaplacianShot [75] also exploits the inherent structure of the data through a graph-Laplacian clustering, which discourages disparate class predictions for samples with close features, while matching each query set point to the nearest support prototype. Alternative approaches propose directly learning the class prototypes. For instance, Transductive Fine-Tuning (TF) [13] uses the prediction entropy on the query samples as a regularization term, while TIM and its variants [5, 58] employ the mutual information between the query samples and their predictions. BD-CSPN [36] refines the class prototypes by reducing the feature biases between the support set and the most confident query samples. An additional group of methods performs clustering in the feature space, for instance, by solving an optimal transport problem like PT-MAP [24], by projecting features into sub-spaces to facilitate clustering [74], or by revisiting the standard K-means with an additional partition-complexity regularizer to control the number of predicted classes [43].

Zero- and few-shot learning in VLMs. Thanks to their extensive pre-training, VLMs exhibit stronger generalization capabilities than vision-only models but may also fail [49, 68, 56]. In response, substantial recent efforts have been directed towards using their general knowledge and adapting them on more specific tasks [62, 72, 69]. Arguably, the most popular strategy is prompt tuning [34], which is explored both in unsupervised [42, 15, 40, 1] and few-shot [72, 71, 39, 12, 64, 6, 73, 8, 9, 29, 30] settings. The pioneering work, CoOp [72], updates input text-prompt tokens by leveraging the context provided by the few labeled samples (i.e., the support set). Building on this success, various strategies have been developed to enhance this approach, especially through additional regularization. For instance, ProGrad [73] guides the prompts towards the original hand-crafted ones by gradient projection. Prompt tuning has also been explored in the zero-shot setting, e.g., using the predictive confidence to generate pseudo-labels [25, 40] [40]. Despite its popularity, prompt tuning remains tedious in terms of computations, due to the many back-propagations through the text encoder. This challenge is compounded in the recent developments, which introduce visual tokens [29, 30] alongside the text tokens. In contrast, there has been limited efforts so far in developing black-box methods [47, 17, 16, 65, 61], which only access the final embedding states. These methods often rely on the so-called adapters [23], like Tip-Adapter(-F) [69], which adds a classifier at the output of the vision encoder, in the form of a cache model involving the few-shot samples. Lately, a strong baseline based on GDA clustering [61] demonstrates VLMs’ adaptation abilities with a simple Gaussian hypothesis on the embedding space.

Despite the growing interest in unsupervised, zero-shot and few-shot learning for VLMs, the transductive-inference paradigm has not been explored so far in this new multi-modal context, except the very recent work in [44], which was deployed for small-size tasks ($\approx 10^2$ test samples). However, the method in [44] may not be computationally tractable to large-scale query sets, due to expensive inner loops for estimating the Dirichlet distribution’s parameters. This paper provides a computationally efficient solution, which can scale up to large target datasets (such as ImageNet), while being easily amenable as a plug-and-play module on top of state-of-the-art inductive methods.

3 TransCLIP: Transduction for Vision-Language Models

In this section, we describe our objective function for transductive inference in vision-language models, and derive a block majorize-minimize (BMM) algorithm for minimizing it, with guaranteed convergence and decoupled sample-assignment updates. When dealing with a zero-shot classification problem based on a vision-language model, such as CLIP, and given a set of K candidate classes, one creates textual descriptions, the so-called prompts [37], each corresponding to a class, e.g., $\mathbf{c}_k = \text{a photo of a [kth class name]}$, $k = 1, \dots, K$. Let $\mathbf{t}_k = \theta_t(\mathbf{c}_k)$ denotes the corresponding

normalized (unit hypersphere) embedding representation, with θ_t representing the language encoder. Similarly, each test image \mathbf{x}_i , $i = 1, \dots, N$, is projected onto a normalized embedding space of the same dimension, using visual encoder θ_v : $\mathbf{f}_i = \theta_v(\mathbf{x}_i)$. In the standard inductive zero-shot inference, classification of a given image \mathbf{x}_i is done by evaluating the cosine similarity between these two encoded modalities and predicting the class corresponding to the most similar text embedding: $\hat{k} = \operatorname{argmax}_k \mathbf{f}_i^\top \mathbf{t}_k$. Furthermore, one can compute pseudo-labels corresponding to these zero-shot predictions by applying the softmax function with a temperature scaling³ τ , which yields the following probability-simplex vector for each sample:

$$\hat{\mathbf{y}}_i = (\hat{y}_{i,k})_{1 \leq k \leq K} \in \Delta_K; \quad \hat{y}_{i,k} = \frac{\exp(\tau \mathbf{f}_i^\top \mathbf{t}_k)}{\sum_j \exp(\tau \mathbf{f}_i^\top \mathbf{t}_j)} \quad (1)$$

where Δ_K denotes the probability simplex. Let $\mathcal{D} = \{i \in \mathbb{N} : 1 \leq i \leq N\} = \mathcal{S} \cup \mathcal{Q}$ denotes the samples indices of the target dataset, with \mathcal{Q} the set of unlabeled *query* samples indices, i.e., those for which we want to make a prediction, and \mathcal{S} the set of labeled *support* samples indices in the few-shot setting.

Note that, in the zero-shot setting, $\mathcal{S} = \emptyset$. We define a Gaussian Mixture Model-clustering (GMM) term in our objective function by modeling the likelihood of these target data as a balanced mixture of multivariate Gaussian distributions, each representing a class k and parameterized by mean vector $\boldsymbol{\mu}_k$ and a diagonal covariance matrix $\boldsymbol{\Sigma}$:

$$p_{i,k} = \Pr(\mathbf{f}_i, k; \boldsymbol{\mu}_k, \boldsymbol{\Sigma}) \propto \det(\boldsymbol{\Sigma})^{-\frac{1}{2}} \exp\left(-\frac{1}{2}(\mathbf{f}_i - \boldsymbol{\mu}_k)^\top \boldsymbol{\Sigma}^{-1}(\mathbf{f}_i - \boldsymbol{\mu}_k)\right)$$

Notation $p_{i,k}$ is introduced here to simplify the equations in the sequel. Notice that, unlike standard GMMs, we deploy a common diagonal covariance matrix $\boldsymbol{\Sigma}$ across all classes. Interestingly, in our experiments, we found this simplifying choice improves the performance while reducing the computational load as there are substantially fewer parameters to learn. This is particularly the case when dealing with large numbers of classes as in large-scale target datasets such as ImageNet.

3.1 Proposed objective function

Our objective function depends on two types of variables: (i) Sample-to-class assignment variables within the probability simplex: $\mathbf{z}_i = (z_{i,k})_{1 \leq k \leq K} \in \Delta_K$, $i \in \mathcal{Q}$; and (ii) GMM parameters $\boldsymbol{\mu} = (\boldsymbol{\mu}_k)_{1 \leq k \leq K}$ and $\boldsymbol{\Sigma}$. We propose to minimize

the following objective, which integrates a GMM-clustering term, a Laplacian regularizer and a Kullback-Leibler (KL) divergence penalty encoding the text-encoder knowledge and guiding the transductive learning process:

$$\mathcal{L}_{\text{ZERO-SHOT}}(\mathbf{z}, \boldsymbol{\mu}, \boldsymbol{\Sigma}) = \underbrace{-\frac{1}{|\mathcal{Q}|} \sum_{i \in \mathcal{Q}} \mathbf{z}_i^\top \log(\mathbf{p}_i)}_{\text{GMM clustering}} - \underbrace{\sum_{i \in \mathcal{D}} \sum_{j \in \mathcal{D}} w_{ij} \mathbf{z}_i \mathbf{z}_j}_{\text{Laplacian reg.}} + \underbrace{\sum_{i \in \mathcal{Q}} \text{KL}_\lambda(\mathbf{z}_i || \hat{\mathbf{y}}_i)}_{\text{Text knowledge}} \quad (2)$$

where $\mathbf{p}_i = (p_{i,k})_{1 \leq k \leq K} \in \Delta_K$ concatenates the GMM probabilities, $w_{i,j}$ denotes some measure of affinity between visual embeddings \mathbf{f}_i and \mathbf{f}_j , and the sample-wise parameterized⁴ KL terms are given by:

$$\text{KL}_\lambda(\mathbf{z}_i || \hat{\mathbf{y}}_i) = \mathbf{z}_i^\top \log \mathbf{z}_i - \lambda \mathbf{z}_i^\top \log \hat{\mathbf{y}}_i, \quad i \in \mathcal{Q}; \quad \lambda > 0 \quad (3)$$

In the following, we describe the effect of each term in our objective function in (2):

- **GMM-based clustering:** This unsupervised-learning term is akin to the GMM-based maximum-likelihood estimation objective in the standard EM algorithm [3]. By taking the negative logarithm, its minimization corresponds to maximizing the likelihood of the data. It can also be viewed as a probabilistic generalization of the K-means clustering objective [28]. Indeed, assuming $\boldsymbol{\Sigma}$ is the identity matrix reduces the first term in (2) to the K-means objective.

³Note that each CLIP version comes with a temperature scaling factor τ , which is optimized along with the learnable parameters during pre-training.

⁴Notice that, for $\lambda = 1$, the expression in (3) corresponds to the KL divergence.

- **Laplacian regularization:** The second term in (2) is the Laplacian regularizer, widely used in the context of graph/spectral clustering [55] and semi-supervised learning [7]. This term encourages nearby samples in the visual-embedding space (i.e., pairs of samples with high affinity $w_{i,j}$) to have similar \mathbf{z} assignments. In our case, we propose to build non-negative affinities based on the cosine similarities as $w_{ij} = \max(0, \mathbf{f}_i^\top \mathbf{f}_j)$. The max operator ensures that the $|\mathcal{D}|$ -by- $|\mathcal{D}|$ affinity matrix $\mathbf{W} = [w_{i,j}]$ is positive semi-definite (PSD). As we see below, this PSD condition is important to obtain a convergent Majorize-Minimize optimizer with decoupled (parallel) sample-wise updates for the \mathbf{z} -assignments, yielding a highly efficient transduction for large-scale target datasets (such as ImageNet).
- **Text-guided KL divergence:** This term is dedicated to vision-language models and, as we will see in our experiments (ablation studies in Tables 4 and 6), has a substantial effect on performance. It encourages the prediction not to deviate significantly from the zero-shot predictions, thereby providing text supervision to the other two unsupervised-learning terms. Furthermore, being convex over \mathbf{z}_i , $i \in \mathcal{Q}$, this term facilitates the optimization of the objective w.r.t the assignment variables.

3.2 Extension to the few-shot setting

Our zero-shot formulation naturally extends to the few-shot setting. We integrate supervision from the labeled-support samples, in the form of a cross-entropy, which corresponds to minimizing the following overall loss:

$$\mathcal{L}_{\text{FEW-SHOT}}(\mathbf{z}, \boldsymbol{\mu}, \boldsymbol{\Sigma}) = -\frac{\gamma}{|\mathcal{S}|} \sum_{i \in \mathcal{S}} \mathbf{z}_i^\top \log(\mathbf{p}_i) + \mathcal{L}_{\text{ZERO-SHOT}}(\mathbf{z}, \boldsymbol{\mu}, \boldsymbol{\Sigma}) \quad (4)$$

Note that, in the first term, the \mathbf{z}_i are fixed, with $\mathbf{z}_i = \mathbf{y}_i$, $i \in \mathcal{S}$ and \mathbf{y}_i the one-hot ground-truth label associated with the corresponding shot.

3.3 Block Majorize-Minimize (BMM) optimization

As our objective depends on three types of variables (\mathbf{z} , $\boldsymbol{\mu}$, $\boldsymbol{\Sigma}$), we proceed with a BMM procedure, alternating three sub-step optimizers. Each sub-step optimizes over one block of variables while the other two are fixed, ensuring the overall objective does not increase. Importantly, the obtained \mathbf{z} -updates (Eq. (5)) are decoupled, yielding computationally efficient transduction for large-scale datasets. Also, our overall procedure is guaranteed to converge (Theorem 1).

Majorize-Minimize (MM) with respect to the \mathbf{z} -block When $\boldsymbol{\mu}$ and $\boldsymbol{\Sigma}$ are fixed, both the GMM- and KL-based terms are convex w.r.t \mathbf{z}_i . However, the Laplacian term is concave⁵ (for PSD matrix \mathbf{W}). Therefore, we proceed with inner iterations, each minimizing a linear and tight upper bound, the so-called majorizing function in the MM-optimization literature [32, 21], which guarantees the overall objective does not increase. To obtain the tight linear bound, let us write the Laplacian term conveniently in the following matrix form: $\mathbf{z}^\top \boldsymbol{\Psi} \mathbf{z}$, with $\boldsymbol{\Psi} = -\mathbf{W} \otimes \mathbf{I}$, where \otimes denotes the Kronecker product and \mathbf{I} is the $N \times N$ identity matrix. Note that $\boldsymbol{\Psi}$ is negative semi-definite for a positive semi-definite \mathbf{W} . Therefore, $\mathbf{z}^\top \boldsymbol{\Psi} \mathbf{z}$ is a concave function with respect to \mathbf{z} , and its first-order approximation at current solution \mathbf{z}^l (l being the iteration index) gives the following tight⁶ upper bound on the Laplacian term:

$$\mathbf{z}^\top \boldsymbol{\Psi} \mathbf{z} \leq (\mathbf{z}^l)^\top \boldsymbol{\Psi} \mathbf{z}^l + (\boldsymbol{\Psi} \mathbf{z}^l)^\top (\mathbf{z} - \mathbf{z}^l)$$

Replacing the quadratic Laplacian term by this linear bound yields a majorizing function on our overall objective. Importantly, this majorizing function is a sum of decoupled objectives, each corresponding to one assignment variable \mathbf{z}_i , yielding a highly efficient optimizer for large-scale target datasets. Indeed, using simplex constraints $\mathbf{z}_i \in \Delta_K$, $i \in \mathcal{Q}$, and solving the Karush-Kuhn-Tucker (KKT) conditions independently for each \mathbf{z}_i , we obtain the following decoupled update rules for the \mathbf{z} -block:

$$\mathbf{z}_i^{(l+1)} = \frac{\hat{\mathbf{y}}_i^\lambda \odot \exp(\log(\mathbf{p}_i) + \sum_{j \in \mathcal{D}} w_{ij} \mathbf{z}_j^{(l)})}{(\hat{\mathbf{y}}_i^\lambda \odot \exp(\log(\mathbf{p}_i) + \sum_{j \in \mathcal{D}} w_{ij} \mathbf{z}_j^{(l)}))^\top \mathbb{1}_K} \quad (5)$$

⁵This makes the overall sub-problem non-convex and there is no closed-form solution.

⁶“Tight” means that the upper bound is equal to the original objective at the current solution \mathbf{z}^l .

Closed-form updates of $\boldsymbol{\mu}$ and $\boldsymbol{\Sigma}$ When both \mathbf{z} and $\boldsymbol{\Sigma}$ are fixed, our objective in (4) is convex. It can be minimized by setting its gradient w.r.t each $\boldsymbol{\mu}_k$ to zero, which yields the following closed-form updates:

$$\boldsymbol{\mu}_k = \frac{\frac{\gamma}{|\mathcal{S}|} \sum_{i \in \mathcal{S}} z_{i,k} \mathbf{f}_i + \frac{1}{|\mathcal{Q}|} \sum_{i \in \mathcal{Q}} z_{i,k} \mathbf{f}_i}{\frac{\gamma}{|\mathcal{S}|} \sum_{i \in \mathcal{S}} z_{i,k} + \frac{1}{|\mathcal{Q}|} \sum_{i \in \mathcal{Q}} z_{i,k}} \quad (6)$$

Similarly, when both \mathbf{z} and $\boldsymbol{\mu}$ are fixed, the following closed-form updates minimize the overall objective w.r.t $\boldsymbol{\Sigma}$:

$$\text{diag}(\boldsymbol{\Sigma}) = \frac{\frac{\gamma}{|\mathcal{S}|} \sum_{i \in \mathcal{S}} \sum_k z_{i,k} (\mathbf{f}_i - \boldsymbol{\mu}_k)^2 + \frac{1}{|\mathcal{Q}|} \sum_{i \in \mathcal{Q}} \sum_k z_{i,k} (\mathbf{f}_i - \boldsymbol{\mu}_k)^2}{\gamma + 1} \quad (7)$$

The complete procedure is summarized in Appendix B. Note that, after convergence, we use the sample-to-class assignment variables \mathbf{z}_i as predictions for each sample i of the query set \mathcal{Q} .

3.4 Convergence

Our optimizer can be viewed as an instance of the general Block Majorize-Minimize paradigm for optimization [50], which optimizes a majorizing function for each block of variables. The convergence of general BMM procedures is well studied in the optimization community [50]. Indeed, under certain conditions (such as the strong convexity of the block-wise majorizing functions), we can establish convergence of our procedure using the following result (more details in Appendix A):

Theorem 1 (Convergence of BMM [50]) *Assume that, for each block, the majorizing function is quasi-convex, and its first-order behavior is the same as the original objective locally. Furthermore, assume that the sub-problem solved for each block has a unique solution. Then, every limit point of the iterates generated by BMM is a coordinate-wise minimum of the overall objective.*

4 Experiments

Datasets. Following the setting of previous works [72, 42], we assess TransCLIP on ImageNet [11] and ten datasets for fine-grained classification of scenes (SUN397 [63]), aircraft types (Aircraft [41]), satellite imagery (EuroSAT [18]), automobiles (Cars [31]), food items (Food [4]), pet breeds (Pets [48]), flowers (Flowers [46]), general objects (Caltech101 [14]), textures (DTD [10]) and human actions (UCF101 [53]). We additionally measure performance on four variants of ImageNet (Adversarial [20], ImageNetV2 [51], Rendition [19], Sketch [60]). Numerical results are reported in terms of the top-1 accuracy with the ViT-B/16 encoder, averaged over three random seeds.

Benchmarks. We aim to show the breadth of potential applications of transduction in the context of VLMs. Notably, employing supervised fine-tuning, followed by transduction with TransCLIP on the unlabeled test samples, emerges as a powerful and efficient solution. This is particularly convenient when the labeled samples (the support set) and/or computational power are not accessible at inference (i.e., test) time⁷. To this end, we first study the applicability of our zero-shot formulation TransCLIP-ZS (Eq. (2)) across three settings: (i) on top of inductive *zero-shot* learning and popular *few-shot* learning methods; (ii) on top of 16-shot ImageNet pretraining for *cross-dataset* transferability, and (iii) on top of 16-shot ImageNet pretraining for *domain generalization* on the four ImageNet variants. Secondly, we compare our few-shot extension TransCLIP-FS (Eq. (4)) to transductive few-shot learning methods. As for TransCLIP-ZS, we operate in a black-box setting (i.e., using only the output embeddings, without training the model parameters).

Implementation details. The main component of our transductive formulation is the text-guided KL divergence penalty. We fix $\lambda = 1$ for all our zero-shot experiments (see ablation study in Table 6), and $\lambda = 0.5$ in all the few-shot experiments to reduce the impact of the text-driven regularization. Another component of our optimization problem is the Laplacian regularization, which enforces consistent predictions for close instances. We truncate the affinity matrix to the 3 nearest-neighbors, making it sparse. $\boldsymbol{\mu}$ is initialized with the top-8 most confident samples of each class for the zero-shot setting. For the few-shot setting, we use the class-wise average over the shot embeddings.

⁷This application is hardly discussed in the transductive literature. We make all zero-shot- and few-shot text and image embeddings publicly available, to ease future works without resorting to heavy computations.

Table 1: TransCLIP atop inductive vision-language zero-shot and popular few-shot methods.

Method	Target											Average
	ImageNet	SUN397	Aircraft	EuroSAT	StanfordCars	Food101	Pets	Flower102	Caltech101	DTD	UCF101	
0-shot												
CLIP-ViT-B/16	66.6	62.5	24.7	48.3	65.6	85.9	89.1	70.7	93.2	43.5	67.5	65.3
+ TransCLIP-ZS	70.3 _{+3.7}	68.9 _{+6.3}	26.9 _{+2.2}	65.1 _{+16.8}	69.4 _{+3.8}	87.1 _{+1.2}	92.6 _{+3.5}	76.7 _{+5.9}	92.7 _{-0.5}	49.5 _{+6.0}	74.4 _{+6.9}	70.3 _{+5.1}
1-shot												
CoOp (ucv ²³)	65.7	66.9	20.7	56.4	67.6	84.3	90.2	78.2	92.5	50.1	71.2	67.6
+ TransCLIP-ZS	69.3 _{+3.6}	71.5 _{+4.6}	23.8 _{+3.1}	65.3 _{+8.9}	71.9 _{+4.3}	86.3 _{+2.0}	91.9 _{+1.8}	89.8 _{+11.5}	93.8 _{+1.3}	55.4 _{+5.4}	77.7 _{+6.5}	72.4 _{+4.8}
TIP-Adapter-F (ccv ²³)	69.5	67.2	28.8	67.8	67.1	85.8	90.6	83.7	94.0	51.6	73.4	70.9
+ TransCLIP-ZS	72.0 _{+2.5}	71.8 _{+4.6}	30.7 _{+1.9}	76.9 _{+9.1}	71.0 _{+3.9}	86.9 _{+1.1}	93.1 _{+2.4}	92.8 _{+9.1}	93.5 _{-0.5}	57.7 _{+6.1}	80.0 _{+6.7}	75.1 _{+4.3}
PLOT (aclr ²³)	66.9	67.0	28.9	72.8	68.5	84.9	91.9	81.8	94.0	52.8	74.7	71.3
+ TransCLIP-ZS	75.8 _{+8.9}	70.3 _{+3.3}	28.1 _{-0.8}	78.8 _{+6.0}	70.0 _{+1.6}	85.3 _{+0.4}	91.1 _{-0.8}	93.2 _{+11.4}	94.0 _{-0.0}	56.7 _{+3.9}	81.4 _{+6.7}	75.0 _{+3.7}
TaskRes (cvpr ²³)	69.6	68.1	31.2	65.6	69.1	84.5	90.2	81.6	93.6	53.4	71.8	70.8
+ TransCLIP-ZS	72.0 _{+2.5}	72.5 _{+4.4}	31.4 _{+0.2}	73.7 _{+8.1}	71.6 _{+2.4}	86.5 _{+2.0}	91.6 _{+1.5}	90.7 _{+9.1}	94.0 _{+0.4}	59.4 _{+6.0}	76.4 _{+4.6}	74.5 _{+3.7}
ProGrad (ccv ²³)	67.0	67.0	28.7	57.0	68.2	84.9	91.4	80.8	93.5	52.8	73.3	69.5
+ TransCLIP-ZS	70.1 _{+3.1}	71.6 _{+4.6}	30.5 _{+1.8}	70.9 _{+13.9}	72.3 _{+4.1}	86.5 _{+1.6}	92.7 _{+1.4}	91.5 _{+10.7}	94.1 _{+0.7}	57.9 _{+5.1}	79.3 _{+6.1}	74.3 _{+4.8}
4-shot												
CoOp (ucv ²³)	68.8	69.7	30.8	69.6	74.4	84.5	92.5	92.2	94.5	59.4	71.2	74.0
+ TransCLIP-ZS	71.4 _{+2.6}	73.3 _{+3.5}	33.1 _{+2.3}	77.2 _{+7.5}	77.7 _{+3.2}	86.5 _{+1.9}	93.6 _{+1.1}	95.3 _{+3.1}	95.1 _{+0.6}	63.0 _{+3.6}	81.8 _{+4.3}	77.1 _{+3.1}
TIP-Adapter-F (ccv ²³)	70.7	70.8	35.7	76.8	74.1	86.5	91.9	92.1	94.8	59.8	78.1	75.6
+ TransCLIP-ZS	72.7 _{+1.9}	74.4 _{+3.5}	36.1 _{+0.5}	79.7 _{+2.9}	75.9 _{+1.8}	87.4 _{+0.9}	93.2 _{+1.3}	95.5 _{+3.3}	95.1 _{-0.3}	64.0 _{+4.2}	83.3 _{+5.2}	77.9 _{+2.3}
PLOT (aclr ²³)	70.0	71.8	34.8	84.7	76.6	83.5	92.8	93.2	94.9	61.0	79.7	76.6
+ TransCLIP-ZS	77.2 _{+7.2}	73.5 _{+1.7}	33.9 _{-0.9}	81.8 _{-2.9}	75.8 _{-0.8}	85.6 _{-2.2}	92.5 _{-0.3}	95.8 _{-2.6}	94.8 _{-0.1}	63.6 _{+2.6}	83.3 _{-3.6}	78.0 _{+1.4}
TaskRes (cvpr ²³)	71.0	72.8	33.3	73.8	78.1	86.1	91.9	85.0	94.9	59.7	75.5	74.6
+ TransCLIP-ZS	73.0 _{+2.0}	75.3 _{+2.5}	34.4 _{+1.1}	78.1 _{+4.4}	77.2 _{-1.1}	87.3 _{+1.2}	93.0 _{+1.1}	92.4 _{+7.4}	95.1 _{+0.2}	64.3 _{+4.6}	79.2 _{+3.7}	77.2 _{+2.7}
ProGrad (ccv ²³)	70.2	71.7	34.0	69.5	75.0	85.4	92.0	91.1	94.4	59.8	77.9	74.6
+ TransCLIP-ZS	72.3 _{+2.1}	75.0 _{+3.3}	35.3 _{+1.6}	74.9 _{+5.3}	77.9 _{+2.9}	87.0 _{+1.5}	93.7 _{+1.7}	95.3 _{+4.2}	95.1 _{+0.8}	64.8 _{+5.1}	83.3 _{+5.4}	77.7 _{+3.1}
16-shot												
CoOp (ucv ²³)	71.9	74.9	43.3	85.0	82.8	84.2	91.9	96.8	95.8	69.7	83.1	79.9
+ TransCLIP-ZS	73.3 _{+1.4}	76.6 _{+1.8}	42.9 _{-0.4}	86.0 _{+1.0}	83.0 _{+0.2}	86.3 _{+2.1}	93.2 _{+1.2}	97.5 _{+0.8}	95.9 _{-0.1}	71.3 _{+1.7}	85.4 _{+2.3}	81.1 _{+1.1}
TIP-Adapter-F (ccv ²³)	73.3	76.0	44.6	85.9	82.3	86.8	92.6	96.2	95.7	70.8	83.9	80.7
+ TransCLIP-ZS	74.2 _{+0.9}	76.8 _{+0.8}	44.9 _{-0.3}	85.2 _{-0.7}	82.7 _{+0.4}	87.4 _{+0.6}	93.5 _{+0.9}	96.9 _{+0.7}	95.7 _{-0.1}	69.2 _{-1.5}	85.6 _{+1.7}	81.1 _{+0.4}
PLOT (aclr ²³)	72.5	76.0	46.8	92.1	84.6	85.6	92.5	97.1	96.0	71.1	84.8	81.7
+ TransCLIP-ZS	77.8 _{+5.3}	75.0 _{-1.0}	41.8 _{-4.9}	84.6 _{-7.5}	79.6 _{-4.9}	85.9 _{+0.2}	92.2 _{-0.4}	97.3 _{+0.1}	95.0 _{-1.0}	68.7 _{-2.4}	70.9 _{+0.9}	80.3 _{-1.4}
TaskRes (cvpr ²³)	73.0	76.0	44.8	80.7	83.5	86.9	92.5	97.3	95.9	70.9	83.4	80.5
+ TransCLIP-ZS	74.3 _{+1.0}	76.9 _{+0.8}	43.6 _{-1.2}	80.5 _{-0.3}	82.8 _{-0.7}	87.5 _{+0.6}	92.9 _{+0.4}	97.6 _{+0.3}	96.0 _{+0.1}	70.2 _{-0.7}	86.2 _{+2.8}	80.8 _{+0.3}
ProGrad (ccv ²³)	72.1	75.1	42.8	83.6	82.9	85.8	92.9	96.6	95.9	68.9	82.6	79.9
+ TransCLIP-ZS	73.5 _{+1.4}	76.8 _{+1.7}	42.8 _{-0.0}	83.7 _{+0.2}	83.1 _{+0.2}	87.2 _{+1.3}	93.7 _{+0.8}	97.4 _{+0.8}	96.0 _{+0.1}	71.4 _{+2.5}	86.1 _{+3.4}	81.1 _{+1.1}

Table 2: Cross-Dataset transferability evaluation. Few-shot learning methods are trained on 16-shot ImageNet and evaluate on the ten other fine-grained datasets. Average excludes ImageNet.

Method	Target											Average
	ImageNet	SUN397	Aircraft	EuroSAT	StanfordCars	Food101	Pets	Flower102	Caltech101	DTD	UCF101	
Cross-Dataset												
CoOp (ucv ²³)	71.9	62.0	15.7	44.6	62.1	84.3	88.3	67.1	92.7	39.5	64.1	62.0
+ TransCLIP-ZS	73.3 _{+1.4}	67.4 _{+5.4}	17.1 _{+1.4}	54.5 _{+9.9}	66.8 _{+4.8}	86.3 _{+2.0}	89.4 _{+1.1}	74.2 _{+7.2}	93.4 _{+0.7}	42.1 _{+2.6}	69.9 _{+5.7}	66.1 _{+4.1}
CoCoOp (cvpr ²³)	71.1	67.0	22.7	44.6	64.9	86.2	90.7	71.6	93.9	45.2	68.8	65.6
+ TransCLIP-ZS	76.8 _{+5.7}	69.6 _{+2.7}	22.6 _{-0.1}	59.2 _{+14.6}	67.0 _{+2.1}	85.4 _{-0.8}	89.8 _{-0.9}	79.0 _{+7.4}	94.3 _{+0.3}	50.6 _{+5.4}	74.5 _{+5.7}	69.2 _{+3.6}
MaPLE (cvpr ²³)	70.5	67.3	24.4	45.8	65.7	86.4	90.4	72.0	93.7	46.3	68.7	66.1
+ TransCLIP-ZS	76.6 _{+6.1}	69.8 _{+2.5}	24.5 _{+0.2}	59.5 _{+13.7}	66.8 _{+1.2}	85.4 _{-1.0}	89.7 _{-0.7}	78.0 _{+6.0}	94.3 _{+0.6}	49.4 _{+3.1}	74.4 _{+5.6}	69.2 _{+3.1}
ProGrad (ccv ²³)	72.1	63.9	21.6	38.9	64.0	85.9	90.2	67.8	92.9	43.2	65.9	63.4
+ TransCLIP-ZS	73.5 _{+1.4}	68.6 _{+4.7}	22.7 _{+1.1}	55.2 _{+16.4}	67.9 _{+3.8}	87.0 _{+1.2}	91.3 _{+1.1}	73.9 _{+6.1}	94.0 _{+1.1}	46.6 _{+3.4}	73.5 _{+7.6}	68.1 _{+4.6}
PromptSRC (ccv ²³)	71.4	67.3	24.1	45.0	65.6	86.5	90.1	70.5	93.8	46.2	68.9	65.8
+ TransCLIP-ZS	76.9 _{+5.5}	69.9 _{+2.6}	24.9 _{+0.8}	59.4 _{+14.4}	67.6 _{+2.0}	85.3 _{-1.2}	89.4 _{-0.7}	76.7 _{+6.2}	94.2 _{+0.4}	51.1 _{+5.0}	76.0 _{+7.0}	69.4 _{+3.7}

Table 3: Domain Generalization evaluation with improved manual prompting strategy (custom templates are given in Table 23b), 16-shot prompt-tuning and 16-shot adapter.

Method	Source	Target					Average	Average OOD
	ImageNet	Adversarial	ImageNetV2	Rendition	Sketch			
0-shot								
CLIP-ViT-B/16 w/ a photo of a	66.6	47.9	60.6	73.8	46.0	59.0	57.1	
+ TransCLIP-ZS	70.3 _{+3.7}	49.5 _{+1.7}	62.3 _{+1.7}	75.0 _{+1.3}	49.7 _{+3.7}	61.4 _{+2.4}	59.2 _{+2.1}	
CLIP-ViT-B/16 w/ custom templates	68.8	50.6	62.3	77.8	48.4	61.6	59.8	
+ TransCLIP-ZS	71.5 _{+2.7}	52.1 _{+1.4}	63.4 _{+1.1}	78.1 _{+0.2}	51.1 _{+2.7}	63.2 _{+1.6}	61.1 _{+1.3}	
Domain G.								
CLIP-ViT-B/16 w/ prompt tuning (CoOp)	71.9	49.4	64.1	75.1	47.2	61.5	59.0	
+ TransCLIP-ZS	73.3 _{+1.4}	50.8 _{+1.4}	64.6 _{+0.5}	75.8 _{+0.7}	50.3 _{+3.1}	63.0 _{+1.5}	60.4 _{+1.4}	
CLIP-ViT-B/16 w/ adapter (TaskRes)	73.0	50.3	65.6	77.8	49.2	63.2	60.7	
+ TransCLIP-ZS	74.1 _{+1.1}	51.9 _{+1.6}	65.4 _{-0.2}	78.4 _{+0.6}	51.6 _{+2.4}	64.3 _{+1.1}	61.8 _{+1.1}	

4.1 Main results

Transduction improvements. Table 1 and 2 demonstrate the advantages of our transductive approach in zero-shot, few-shot, and cross-dataset transferability. TransCLIP enhances the zero-shot top-1 accuracy by over 5% and popular few-shot methods by 4% (1-shot) on average, without the need for additional labels. Table 3 further highlights that TransCLIP can be applied on top of prompt tuning and adapter fine-tuning solutions, enhancing performance for both in-domain and domain generalization tasks. However, we observe in Table 1 that transductive gains sometimes decrease with the number of shots, presumably because data structure information can be partially captured in

Table 4: Transductive few-shot learning evaluation. *w/o text* denotes $\lambda = 0$ in Eq. (3).

Shots	Method	ImageNet	SUN	Aircraft	EuroSAT	Cars	Food	Pets	Flowers	Caltech	DTD	UCF	Average
0	CLIP-ViT-B/16	66.6	62.5	24.7	48.3	65.6	85.9	89.1	70.7	93.2	43.5	67.5	65.3
1	TF [13]	29.7	38.1	19.2	46.0	32.5	43.5	38.2	67.8	75.5	31.6	48.8	42.8
	BD-CSPN [36]	35.4	45.7	22.0	45.7	42.0	54.2	52.9	82.9	83.5	34.7	58.0	50.6
	LaplacianShot [75]	34.9	44.5	22.1	52.1	41.1	53.0	52.2	83.1	83.4	35.8	57.3	50.9
	PT-MAP [24]	40.1	52.6	23.8	59.7	48.4	64.4	61.8	69.4	54.1	41.8	63.5	52.7
	TIM [5]	37.5	48.3	22.8	48.2	44.8	65.7	53.9	86.4	75.1	35.8	62.7	52.8
	TransCLIP-FS <i>w/o text</i>	30.2	43.4	23.7	56.6	41.0	50.9	54.3	83.5	77.7	36.9	54.5	50.2
	TransCLIP-FS	69.8	70.6	29.9	72.5	70.9	87.9	93.8	84.8	93.1	53.3	78.4	73.2
4	TF [13]	51.1	61.0	30.3	64.9	56.8	71.0	65.9	90.9	91.5	53.7	67.9	64.1
	BD-CSPN [36]	53.8	62.5	30.5	64.8	58.5	75.3	72.0	92.5	92.0	52.1	70.9	65.9
	LaplacianShot [75]	53.5	62.5	29.6	74.3	58.5	75.7	73.4	92.8	92.0	52.7	71.7	67.0
	PT-MAP [24]	57.6	68.1	31.2	74.9	63.1	81.1	79.5	76.2	60.2	58.4	73.9	65.8
	TIM [5]	57.4	67.0	32.8	79.3	65.8	83.5	82.3	93.4	88.5	58.1	76.5	71.3
	TransCLIP-FS <i>w/o text</i>	53.9	63.8	34.2	79.4	63.5	76.7	76.7	93.3	92.8	57.0	74.8	69.6
	TransCLIP-FS	70.3	71.9	34.0	79.4	74.0	86.4	91.6	93.6	94.0	61.1	79.1	75.9
16	TF [13]	61.8	70.1	38.3	74.3	71.2	80.7	79.5	95.4	93.6	62.9	76.0	73.1
	BD-CSPN [36]	61.7	69.4	37.7	73.4	70.7	80.2	81.2	94.8	93.3	61.3	76.0	72.7
	LaplacianShot [75]	60.9	68.3	36.1	78.1	69.2	81.2	81.7	94.8	93.1	58.6	76.3	72.6
	PT-MAP [24]	64.0	72.0	37.4	75.6	72.0	82.7	86.1	78.5	63.7	63.7	76.3	70.2
	TIM [5]	67.8	73.6	40.6	83.6	79.5	84.9	88.7	95.4	92.4	67.5	82.1	77.8
	TransCLIP-FS <i>w/o text</i>	65.9	72.6	41.9	81.1	77.0	83.2	86.1	95.2	94.6	65.3	80.0	76.6
	TransCLIP-FS	71.8	74.7	38.6	83.0	79.8	86.9	92.4	94.4	94.0	65.1	82.1	78.4

Table 5: Performance and runtime comparison between TransCLIP and prompt learning solutions on average over ImageNet and the 10 fine-grained classification datasets. UPL* is a transductive adaptation of the original unsupervised procedure in [25], more details in Appendices C.1 and C.5.

(a) Zero-shot setting.			(b) Few-shot setting (4-shot).		
	Performance	Runtime		Performance	Runtime
UPL*	69.8	>150 min	CoOp+UPL*	74.4	>12h
TransCLIP-ZS	70.3	14.4 sec	TransCLIP-FS	75.9	35.3 sec

the shots. These results underline the value of considering the structure of the unlabeled test samples during prediction, especially on top of zero- and low-shot models or when facing domain shifts, an aspect not leveraged by the current zero- and few-shot VLM literature. More detailed results for five different backbone architectures and comparisons with unsupervised non-transductive methods are provided in Appendix C.1 for the zero-shot setting, in Appendix C.2 for TransCLIP on top of popular few-shot methods, in Appendix C.3 for cross-dataset transferability and in Appendix C.4 for domain generalization. *With its hyper-parameters unchanged*, TransCLIP exhibits strong generalization from convolutional networks to transformer-based models, as also depicted in Figure 1.

Transductive few-shot learning. We compare TransCLIP, TransCLIP without text regularization (i.e., $\lambda = 0$) and state-of-the-art transductive few-shot methods. It is important to note that these few-shot methods were primarily developed for vision-centric tasks. Hence, they rely on visual information, omitting the textual elements. This allows us to study the impact of our text-based regularization term. Table 4 shows that incorporating language in the transductive paradigm boosts the performance over vision-only methods. Especially for the 1- to 4-shot settings, our language-driven KL penalty enhances the performance by a large margin on many tasks (e.g., ImageNet, SUN, Cars, DTD). As the number of shots increases, the text-driven penalty becomes less useful, especially for the datasets capitalizing on the visual shots rather than the text-encoder knowledge (e.g., EuroSat and Flowers). Detailed results for five different encoder architectures are provided in Appendix C.5.

Comparison with prompt learning. Following current VLMs literature, adapting the input prompt instead of GMM parameters could be seen as a more straightforward solution. For a fair comparison, we adapt Unsupervised Prompt Learning (UPL) [25] for the transductive setting and reevaluate its main hyper-parameter (see Appendix C.1). It appears clearly that TransCLIP outperforms UPL while being two to three orders of magnitude faster (see Table 5 for runtime and performance comparisons).

Table 6: Analysis on the components and sensitivity to hyper-parameters of TransCLIP-ZS.

(a) Components of the procedure.							(b) Text regularization hyper-parameter λ .				
Update μ	Update Σ	Lapl. w	ImageNet	SUN	Aircraft	EuroSAT	λ	ImageNet	SUN	Aircraft	EuroSAT
X	✓	✓	69.7	67.5	25.5	63.9	0.1	56.3	58.6	26.0	65.5
✓	X	✓	68.7	66.0	25.1	51.6	0.5	69.8	69.3	26.6	65.6
✓	✓	X	69.9	68.8	27.0	64.5	1	70.3	68.9	26.9	65.1
X	X	✓	68.6	65.9	25.2	61.8	2	69.5	67.6	26.2	64.1
✓	✓	✓	70.3	68.9	26.9	65.1	5	68.2	65.2	25.2	51.2

(c) Number of nearest-neighbors.					(d) Impact of an isotropic Σ .				
# neighbors	ImageNet	SUN	Aircraft	EuroSAT		ImageNet	SUN	Aircraft	EuroSAT
3	70.3	68.9	26.9	65.1	Σ (ours)	70.3	68.9	26.9	65.1
5	70.3	68.9	26.8	65.1	Σ isotropic	59.9	64.8	25.0	63.5
10	70.2	68.8	26.9	65.2	Δ	-10.4	-4.1	-1.9	-1.6

4.2 Ablation studies

Components of TransCLIP. We study the impact of the principal components involved in the TransCLIP procedure over four diverse datasets. Table 6a shows that updating μ and Σ allows to significantly boost TransCLIP’s performance. This indicates the importance of having a dynamic parametric model instead of a fixed one. Table 6b demonstrates the critical role of text-driven penalty for TransCLIP in the zero-shot setting. Alongside the prior findings from Table 4, it is evident that incorporating text information is key to the success of TransCLIP and its wide applicability across the zero- and few-shot learning scenarios. The number of nearest-neighbors considered in the Laplacian term (Eq. (2)) does not make a significant difference in TransCLIP’s performance as suggested by Table 6c. However, removing the Laplacian regularization (Table 6a) leads to inferior results on some datasets such as ImageNet and EuroSAT. We choose to consider 3 nearest-neighbors to make the affinity matrix W sparse and reduce memory consumption. We also investigate the diagonal covariance matrix design by restricting it to be isotropic (i.e., $\Sigma = \sigma^2 I_d$ with I_d the identity matrix). Table 6d shows that a non-isotropic Σ performs better without significantly increasing the amount of trainable parameters.

Scaling to larger VLMs. We report TransCLIP-ZS performance on EVA-CLIP 8 billion parameter version [54] (approximately 42 times larger than the CLIP-ViT-B/16). It is worth mentioning that TransCLIP is easily applicable to multi-billion parameter models since it does not necessitate gradient computation or model parameter training (i.e., it only requires the memory needed for single-sample inference because the whole dataset processing can be performed one sample at a time). Table 7 shows that transduction can also bring significant improvements to larger models (details in Appendix C.1).

Table 7: Performance of TransCLIP-ZS for increasingly large VLMs. Relative Δ is the improvement normalized by the zero-shot error: $(\text{Acc}_{\text{TRANSCLIP}} - \text{Acc}_{\text{ZERO-SHOT}}) / (100 - \text{Acc}_{\text{ZERO-SHOT}})$.

	#Params	ImageNet			Average (11 datasets)		
		Zero-shot	w/ TransCLIP-ZS	relative Δ	Zero-shot	w/ TransCLIP-ZS	relative Δ
CLIP-ViT-B/16	177M	66.6	70.3+ 3.7	+11 %	65.3	70.3+ 5.0	+14 %
CLIP-ViT-L/14	427M	72.9	77.2+ 4.3	+16 %	72.5	77.4+ 4.9	+18 %
EVA-CLIP-8B	7.5B	82.5	84.6+ 2.1	+12 %	81.5	85.8+ 4.3	+23 %

5 Conclusion

In this work, we studied the transductive paradigm in the context of Vision-Language Models via TransCLIP. We first showed how TransCLIP can bring transduction to inductive zero-shot and popular few-shot methods, while only working in the output embedding space (i.e., black-box setting). Then, we demonstrated the limitations of current transductive few-shot methods and proposed a simple extension of TransCLIP to incorporate labeled samples. TransCLIP’s text-guided KL divergence term appears as a key factor in its success and future works may consider making it more resilient (e.g., through adaptive class-wise weighting factor) when text prompts are less reliable.

6 Acknowledgments

M. Zanella and B. Gérin are funded by the Walloon region under grant No. 2010235 (ARIAC by DIGITALWALLONIA4.AI). The present research benefited from computational resources made available on Lucia, infrastructure funded by the Walloon Region under grant No. 1910247.

References

- [1] Jameel Abdul Samadh, Mohammad Hanan Gani, Noor Hussein, Muhammad Uzair Khattak, Muhammad Muzammal Naseer, Fahad Shahbaz Khan, and Salman H Khan. Align your prompts: Test-time prompting with distribution alignment for zero-shot generalization. *Advances in Neural Information Processing Systems*, 36, 2024.
- [2] Omer Belhasin, Guy Bar-Shalom, and Ran El-Yaniv. Transboost: Improving the best imagenet performance using deep transduction. *Advances in Neural Information Processing Systems*, 35: 28363–28373, 2022.
- [3] Christopher M Bishop. Pattern recognition and machine learning. *Springer google schola*, 2: 5–43, 2006.
- [4] Lukas Bossard, Matthieu Guillaumin, and Luc Van Gool. Food-101—mining discriminative components with random forests. In *Computer Vision—ECCV 2014: 13th European Conference, Zurich, Switzerland, September 6–12, 2014, Proceedings, Part VI 13*, pages 446–461. Springer, 2014.
- [5] Malik Boudiaf, Imtiaz Ziko, Jérôme Rony, José Dolz, Pablo Piantanida, and Ismail Ben Ayed. Information maximization for few-shot learning. *Advances in Neural Information Processing Systems*, 33:2445–2457, 2020.
- [6] Adrian Bulat and Georgios Tzimiropoulos. Lasp: Text-to-text optimization for language-aware soft prompting of vision & language models. In *Proceedings of the IEEE/CVF Conference on Computer Vision and Pattern Recognition (CVPR)*, pages 23232–23241, June 2023.
- [7] Olivier Chapelle, Bernhard Schlkopf, and Alexander Zien. *Semi-Supervised Learning*. The MIT Press, 1st edition, 2010. ISBN 0262514125.
- [8] Guangyi Chen, Weiran Yao, Xiangchen Song, Xinyue Li, Yongming Rao, and Kun Zhang. Plot: Prompt learning with optimal transport for vision-language models. In *The Eleventh International Conference on Learning Representations*, 2022.
- [9] Eulrang Cho, Jooyeon Kim, and Hyunwoo J Kim. Distribution-aware prompt tuning for vision-language models. In *Proceedings of the IEEE/CVF International Conference on Computer Vision*, pages 22004–22013, 2023.
- [10] Mircea Cimpoi, Subhransu Maji, Iasonas Kokkinos, Sammy Mohamed, and Andrea Vedaldi. Describing textures in the wild. In *Proceedings of the IEEE conference on computer vision and pattern recognition*, pages 3606–3613, 2014.
- [11] Jia Deng, Wei Dong, Richard Socher, Li-Jia Li, Kai Li, and Li Fei-Fei. Imagenet: A large-scale hierarchical image database. In *2009 IEEE Conference on Computer Vision and Pattern Recognition*, pages 248–255, 2009. doi: 10.1109/CVPR.2009.5206848.
- [12] Mohammad Mahdi Derakhshani, Enrique Sanchez, Adrian Bulat, Victor Guilherme Turrissi da Costa, Cees GM Snoek, Georgios Tzimiropoulos, and Brais Martinez. Variational prompt tuning improves generalization of vision-language models. *arXiv preprint arXiv:2210.02390*, 2022.
- [13] Guneet Singh Dhillon, Pratik Chaudhari, Avinash Ravichandran, and Stefano Soatto. A baseline for few-shot image classification. In *International Conference on Learning Representations*, 2019.

- [14] Li Fei-Fei, Rob Fergus, and Pietro Perona. Learning generative visual models from few training examples: An incremental bayesian approach tested on 101 object categories. In *2004 conference on computer vision and pattern recognition workshop*, pages 178–178. IEEE, 2004.
- [15] Chun-Mei Feng, Kai Yu, Yong Liu, Salman Khan, and Wangmeng Zuo. Diverse data augmentation with diffusions for effective test-time prompt tuning. In *Proceedings of the IEEE/CVF International Conference on Computer Vision*, pages 2704–2714, 2023.
- [16] Peng Gao, Shijie Geng, Renrui Zhang, Teli Ma, Rongyao Fang, Yongfeng Zhang, Hongsheng Li, and Yu Qiao. Clip-adapter: Better vision-language models with feature adapters. *International Journal of Computer Vision*, pages 1–15, 2023.
- [17] Ziyu Guo, Renrui Zhang, Longtian Qiu, Xianzheng Ma, Xupeng Miao, Xuming He, and Bin Cui. Calip: Zero-shot enhancement of clip with parameter-free attention. In *Proceedings of the AAAI Conference on Artificial Intelligence*, volume 37, pages 746–754, 2023.
- [18] Patrick Helber, Benjamin Bischke, Andreas Dengel, and Damian Borth. Eurosat: A novel dataset and deep learning benchmark for land use and land cover classification. *IEEE Journal of Selected Topics in Applied Earth Observations and Remote Sensing*, 12(7):2217–2226, 2019.
- [19] Dan Hendrycks, Steven Basart, Norman Mu, Saurav Kadavath, Frank Wang, Evan Dorundo, Rahul Desai, Tyler Zhu, Samyak Parajuli, Mike Guo, et al. The many faces of robustness: A critical analysis of out-of-distribution generalization. In *Proceedings of the IEEE/CVF International Conference on Computer Vision*, pages 8340–8349, 2021.
- [20] Dan Hendrycks, Kevin Zhao, Steven Basart, Jacob Steinhardt, and Dawn Song. Natural adversarial examples. In *Proceedings of the IEEE/CVF Conference on Computer Vision and Pattern Recognition*, pages 15262–15271, 2021.
- [21] Mingyi Hong, Xiangfeng Wang, Meisam Razaviyayn, and Zhi-Quan Luo. Iteration complexity analysis of block coordinate descent methods. *Mathematical Programming*, 163:85–114, 2017.
- [22] Z hong, D Friedman, and D Chen. Factual probing is [mask]: Learning vs. learning to recall. In *Conference of the North American Chapter of the Association for Computational Linguistics (NAACL)*, 2021.
- [23] Neil Houlsby, Andrei Giurgiu, Stanislaw Jastrzebski, Bruna Morrone, Quentin De Laroussilhe, Andrea Gesmundo, Mona Attariyan, and Sylvain Gelly. Parameter-efficient transfer learning for nlp. In *International Conference on Machine Learning*, pages 2790–2799. PMLR, 2019.
- [24] Yuqing Hu, Vincent Gripon, and Stéphane Pateux. Leveraging the feature distribution in transfer-based few-shot learning. In *International Conference on Artificial Neural Networks*, pages 487–499, 2021.
- [25] Tony Huang, Jack Chu, and Fangyun Wei. Unsupervised prompt learning for vision-language models. *arXiv preprint arXiv:2204.03649*, 2022.
- [26] Z Jiang, F Xu, J Araki, and G Neubig. How can we know what language models know. In *Association for Computational Linguistics (ACL)*, 2020.
- [27] Thorsten Joachims. Transductive inference for text classification using support vector machines. In *Proceedings of the Sixteenth International Conference on Machine Learning*, pages 200–209, 1999.
- [28] Michael Kearns, Yishay Mansour, and Andrew Y Ng. An information-theoretic analysis of hard and soft assignment methods for clustering. *Learning in graphical models*, pages 495–520, 1998.
- [29] Muhammad Uzair Khattak, Hanoona Rasheed, Muhammad Maaz, Salman Khan, and Fahad Shahbaz Khan. Maple: Multi-modal prompt learning. In *Proceedings of the IEEE/CVF Conference on Computer Vision and Pattern Recognition*, pages 19113–19122, 2023.

- [30] Muhammad Uzair Khattak, Syed Talal Wasim, Muzammal Naseer, Salman Khan, Ming-Hsuan Yang, and Fahad Shahbaz Khan. Self-regulating prompts: Foundational model adaptation without forgetting. In *Proceedings of the IEEE/CVF International Conference on Computer Vision*, pages 15190–15200, 2023.
- [31] Jonathan Krause, Michael Stark, Jia Deng, and Li Fei-Fei. 3d object representations for fine-grained categorization. In *Proceedings of the IEEE international conference on computer vision workshops*, pages 554–561, 2013.
- [32] Kenneth Lange, David R Hunter, and Ilsoon Yang. Optimization transfer using surrogate objective functions. *Journal of computational and graphical statistics*, 9(1):1–20, 2000.
- [33] Michalis Lazarou, Tania Stathaki, and Yannis Avrithis. Iterative label cleaning for transductive and semi-supervised few-shot learning. In *Proceedings of the IEEE/CVF International Conference on Computer Vision*, pages 8751–8760, 2021.
- [34] Brian Lester, Rami Al-Rfou, and Noah Constant. The power of scale for parameter-efficient prompt tuning. *arXiv preprint arXiv:2104.08691*, 2021.
- [35] Jian Liang, Dapeng Hu, and Jiashi Feng. Do we really need to access the source data? source hypothesis transfer for unsupervised domain adaptation. In *International conference on machine learning*, pages 6028–6039. PMLR, 2020.
- [36] Jinlu Liu, Liang Song, and Yongqiang Qin. Prototype rectification for few-shot learning. In *Computer Vision—ECCV 2020: 16th European Conference, Glasgow, UK, August 23–28, 2020, Proceedings, Part I 16*, pages 741–756. Springer, 2020.
- [37] Pengfei Liu, Weizhe Yuan, Jinlan Fu, Zhengbao Jiang, Hiroaki Hayashi, and Graham Neubig. Pre-train, prompt, and predict: A systematic survey of prompting methods in natural language processing. *ACM Computing Surveys*, 55(9):1–35, 2023.
- [38] Y Liu, J Lee, M Park, S Kim, E Yang, SJ Hwang, and Y Yang. Learning to propagate labels: Transductive propagation network for few-shot learning. In *7th International Conference on Learning Representations, ICLR 2019*, 2019.
- [39] Yuning Lu, Jianzhuang Liu, Yonggang Zhang, Yajing Liu, and Xinmei Tian. Prompt distribution learning. In *Proceedings of the IEEE/CVF Conference on Computer Vision and Pattern Recognition*, pages 5206–5215, 2022.
- [40] Xiaosong Ma, Jie Zhang, Song Guo, and Wenchao Xu. Swapprompt: Test-time prompt adaptation for vision-language models. In *Thirty-seventh Conference on Neural Information Processing Systems*, 2023.
- [41] Subhransu Maji, Esa Rahtu, Juho Kannala, Matthew Blaschko, and Andrea Vedaldi. Fine-grained visual classification of aircraft. *arXiv preprint arXiv:1306.5151*, 2013.
- [42] Shu Manli, Nie Weili, Huang De-An, Yu Zhiding, Goldstein Tom, Anandkumar Anima, and Xiao Chaowei. Test-time prompt tuning for zero-shot generalization in vision-language models. In *NeurIPS*, 2022.
- [43] Ségolène Martin, Malik Boudiaf, Emilie Chouzenoux, Jean-Christophe Pesquet, and Ismail Ayed. Towards practical few-shot query sets: Transductive minimum description length inference. *Advances in Neural Information Processing Systems*, 35:34677–34688, 2022.
- [44] Ségolène Martin, Yunshi Huang, Fereshteh Shakeri, Jean-Christophe Pesquet, and Ismail Ben Ayed. Transductive zero-shot and few-shot clip. In *CVPR 2024—IEEE Conference on Computer Vision and Pattern Recognition*, 2024.
- [45] Zachary Nado, Shreyas Padhy, D Sculley, Alexander D’Amour, Balaji Lakshminarayanan, and Jasper Snoek. Evaluating prediction-time batch normalization for robustness under covariate shift. *arXiv preprint arXiv:2006.10963*, 2020.
- [46] Maria-Elena Nilsback and Andrew Zisserman. Automated flower classification over a large number of classes. In *2008 Sixth Indian conference on computer vision, graphics & image processing*, pages 722–729. IEEE, 2008.

- [47] Yassine Ouali, Adrian Bulat, Brais Matinez, and Georgios Tzimiropoulos. Black box few-shot adaptation for vision-language models. In *Proceedings of the IEEE/CVF International Conference on Computer Vision*, pages 15534–15546, 2023.
- [48] Omkar M Parkhi, Andrea Vedaldi, Andrew Zisserman, and CV Jawahar. Cats and dogs. In *2012 IEEE conference on computer vision and pattern recognition*, pages 3498–3505. IEEE, 2012.
- [49] Alec Radford, Jong Wook Kim, Chris Hallacy, Aditya Ramesh, Gabriel Goh, Sandhini Agarwal, Girish Sastry, Amanda Askell, Pamela Mishkin, Jack Clark, Gretchen Krueger, and Ilya Sutskever. Learning transferable visual models from natural language supervision, 2021.
- [50] Meisam Razaviyayn, Mingyi Hong, and Zhi-Quan Luo. A unified convergence analysis of block successive minimization methods for nonsmooth optimization. *SIAM Journal on Optimization*, 23(2):1126–1153, 2013. doi: 10.1137/120891009. URL <https://doi.org/10.1137/120891009>.
- [51] Benjamin Recht, Rebecca Roelofs, Ludwig Schmidt, and Vaishaal Shankar. Do imagenet classifiers generalize to imagenet? In *International conference on machine learning*, pages 5389–5400. PMLR, 2019.
- [52] T Shin, Logan R. L. IV Razeghi, Y, E Wallace, and S Singh. Autoprompt: Eliciting knowledge from language models with automatically generated prompts. In *Empirical Methods in Natural Language Processing (EMNLP)*, 2020.
- [53] Khurram Soomro, Amir Roshan Zamir, and Mubarak Shah. Ucf101: A dataset of 101 human actions classes from videos in the wild. *arXiv preprint arXiv:1212.0402*, 2012.
- [54] Quan Sun, Jinsheng Wang, Qiyang Yu, Yufeng Cui, Fan Zhang, Xiaosong Zhang, and Xinlong Wang. Eva-clip-18b: Scaling clip to 18 billion parameters, 2024.
- [55] Meng Tang, Dmitrii Marin, Ismail Ben Ayed, and Yuri Boykov. Kernel cuts: Kernel and spectral clustering meet regularization. *International Journal of Computer Vision*, 127:477–511, 2019.
- [56] Vishaal Udandarao, Ameya Prabhu, Adhiraj Ghosh, Yash Sharma, Philip HS Torr, Adel Bibi, Samuel Albanie, and Matthias Bethge. No "zero-shot" without exponential data: Pretraining concept frequency determines multimodal model performance. *arXiv preprint arXiv:2404.04125*, 2024.
- [57] V.N. Vapnik. An overview of statistical learning theory. *IEEE Transactions on Neural Networks*, 10(5):988–999, 1999. doi: 10.1109/72.788640.
- [58] Olivier Veilleux, Malik Boudiaf, Pablo Piantanida, and Ismail Ben Ayed. Realistic evaluation of transductive few-shot learning. *Advances in Neural Information Processing Systems*, 34: 9290–9302, 2021.
- [59] Dequan Wang, Evan Shelhamer, Shaoteng Liu, Bruno Olshausen, and Trevor Darrell. Tent: Fully test-time adaptation by entropy minimization. In *International Conference on Learning Representations*, 2021. URL <https://openreview.net/forum?id=uX13bZLkr3c>.
- [60] Haohan Wang, Songwei Ge, Zachary Lipton, and Eric P Xing. Learning robust global representations by penalizing local predictive power. *Advances in Neural Information Processing Systems*, 32, 2019.
- [61] Zhengbo Wang, Jian Liang, Lijun Sheng, Ran He, Zilei Wang, and Tieniu Tan. A hard-to-beat baseline for training-free clip-based adaptation. In *The Twelfth International Conference on Learning Representations*, 2023.
- [62] Mitchell Wortsman, Gabriel Ilharco, Jong Wook Kim, Mike Li, Simon Kornblith, Rebecca Roelofs, Raphael Gontijo Lopes, Hannaneh Hajishirzi, Ali Farhadi, Hongseok Namkoong, et al. Robust fine-tuning of zero-shot models. In *Proceedings of the IEEE/CVF Conference on Computer Vision and Pattern Recognition*, pages 7959–7971, 2022.
- [63] Jianxiong Xiao, James Hays, Krista A Ehinger, Aude Oliva, and Antonio Torralba. Sun database: Large-scale scene recognition from abbey to zoo. In *2010 IEEE computer society conference on computer vision and pattern recognition*, pages 3485–3492. IEEE, 2010.

- [64] Hantao Yao, Rui Zhang, and Changsheng Xu. Visual-language prompt tuning with knowledge-guided context optimization. In *Proceedings of the IEEE/CVF Conference on Computer Vision and Pattern Recognition*, pages 6757–6767, 2023.
- [65] Tao Yu, Zhihe Lu, Xin Jin, Zhibo Chen, and Xinchao Wang. Task residual for tuning vision-language models. In *Proceedings of the IEEE/CVF Conference on Computer Vision and Pattern Recognition*, pages 10899–10909, 2023.
- [66] Maxime Zanella and Ismail Ben Ayed. Low-rank few-shot adaptation of vision-language models. *arXiv preprint arXiv:2405.18541*, 2024.
- [67] Maxime Zanella and Ismail Ben Ayed. On the test-time zero-shot generalization of vision-language models: Do we really need prompt learning? *arXiv preprint arXiv:2405.02266*, 2024.
- [68] Jingyi Zhang, Jiaying Huang, Sheng Jin, and Shijian Lu. Vision-language models for vision tasks: A survey. *arXiv preprint arXiv:2304.00685*, 2023.
- [69] Renrui Zhang, Wei Zhang, Rongyao Fang, Peng Gao, Kunchang Li, Jifeng Dai, Yu Qiao, and Hongsheng Li. Tip-adapter: Training-free adaption of clip for few-shot classification. In *European Conference on Computer Vision*, pages 493–510. Springer, 2022.
- [70] Dengyong Zhou, Olivier Bousquet, Thomas Lal, Jason Weston, and Bernhard Schölkopf. Learning with local and global consistency. *Advances in neural information processing systems*, 16, 2003.
- [71] Kaiyang Zhou, Jingkang Yang, Chen Change Loy, and Ziwei Liu. Conditional prompt learning for vision-language models. In *IEEE/CVF Conference on Computer Vision and Pattern Recognition (CVPR)*, 2022.
- [72] Kaiyang Zhou, Jingkang Yang, Chen Change Loy, and Ziwei Liu. Learning to prompt for vision-language models. *International Journal of Computer Vision (IJCV)*, 2022.
- [73] Beier Zhu, Yulei Niu, Yucheng Han, Yue Wu, and Hanwang Zhang. Prompt-aligned gradient for prompt tuning. In *Proceedings of the IEEE/CVF International Conference on Computer Vision*, pages 15659–15669, 2023.
- [74] Hao Zhu and Piotr Koniusz. Ease: Unsupervised discriminant subspace learning for transductive few-shot learning. In *Proceedings of the IEEE/CVF Conference on Computer Vision and Pattern Recognition (CVPR)*, pages 9078–9088, June 2022.
- [75] Imtiaz Ziko, Jose Dolz, Eric Granger, and Ismail Ben Ayed. Laplacian regularized few-shot learning. In *International conference on machine learning*, pages 11660–11670. PMLR, 2020.

A More details on convergence

As mentioned in the main paper, our derived block-wise optimization procedure in Eqs. (5), (6) and (7) can be viewed as an instance of the the general Block Majorize-Minimize paradigm for non-convex optimization, also referred to as the Block Successive Minimization (BSUM) method [50]. We update each block of variables, with the other blocks fixed, by minimizing a tight upper bound (majorizing function), thereby guaranteeing the overall objective does not increase at each step. In the steps with respect to $\boldsymbol{\mu}$ and $\boldsymbol{\Sigma}$, we optimize directly the objective in closed-form, which could be also viewed as a particular case of optimizing a tight upper bound. The convergence of the general BSUM procedure is well studied in the optimization community [50]. Indeed, under the following assumptions for each block of variables, one can establish convergence results for the application of BSUM to non-convex problems [50]:

- A1: The majorizing function is a tight upper bound, i.e., equal to the objective at the current solution.
- A2: The first-order behavior of the majorizing function is the same as the original objective locally.

Indeed, when assumptions A1 and A2 are verified for each block, we have the result in Theorem 1 [50].

As for our case of alternating Eqs. (5), (6) and (7), it is straightforward to verify that Assumptions A1 and A2 are satisfied for each block of variables. Furthermore, the majorizing functions are convex and thus quasi-convex. Also, the sub-problem solved for each block has a unique solution. In particular, for the \mathbf{z} -updates, the majorizing function is the sum of a linear and a strongly convex function (the negative entropy). Therefore, it is strongly convex. As for the $\boldsymbol{\mu}$ - and $\boldsymbol{\Sigma}$ -updates, the solutions are obtained in closed form (hence unique).

Algorithm 1 TransCLIP

Require: A set of image embeddings $(\mathbf{f}_i)_{1 \leq i \leq N}$, a set of textual class embeddings $(\mathbf{t}_k)_{1 \leq k \leq K}$, τ the temperature of the CLIP model.

- 1: $w_{i,j} \leftarrow \max(0, \mathbf{f}_i^\top \mathbf{f}_j) \quad \forall i, j$ ▷ Affinity measure, truncated with top-3 values
 - 2: $\hat{\mathbf{y}}_i \leftarrow \varphi(\tau \mathbf{f}_i^\top \mathbf{t}) \quad \forall i$ ▷ Initial predictions, φ the softmax function
 - 3: $\boldsymbol{\mu}_k \leftarrow \text{mean}\{\mathbf{f}_i \text{ s.t. } y = k, i \in \mathcal{S}\}^8 \quad \forall k$ ▷ Class centroids initialization
 - 4: $\text{diag}(\boldsymbol{\Sigma}) \leftarrow \mathbf{1} \frac{1}{d}$ ▷ Covariance matrix initialization, d is the emb. dim.
 - 5: $\mathbf{z}_i \leftarrow \hat{\mathbf{y}}_i \quad \forall i$ ▷ Initial assignments
 - 6: **while** (1), (2) and (3) not converged **do** ▷ Block-wise updates loop
 - 7: **while** (1) not converged **do** ▷ \mathbf{z} -update loop
 - 8: $z_{i,k} \leftarrow \frac{\hat{y}_{i,k}^\lambda \exp(\log(p_{i,k}) + \sum_{j \in \mathcal{D}} w_{ij} z_{j,k})}{\sum_{k'} \hat{y}_{i,k'}^\lambda \exp(\log(p_{i,k'}) + \sum_{j \in \mathcal{D}} w_{ij} z_{j,k'})} \quad \forall i \forall k$ ▷ (1) \mathbf{z} -step
 - 9: **end while**
 - 10: $\boldsymbol{\mu}_k \leftarrow \frac{\frac{1}{|\mathcal{S}|} \sum_{i \in \mathcal{S}} z_{i,k} \mathbf{f}_i + \frac{1}{|\mathcal{Q}|} \sum_{i \in \mathcal{Q}} z_{i,k} \mathbf{f}_i}{\frac{1}{|\mathcal{S}|} \sum_{i \in \mathcal{S}} z_{i,k} + \frac{1}{|\mathcal{Q}|} \sum_{i \in \mathcal{Q}} z_{i,k}} \quad \forall k$ ▷ (2) $\boldsymbol{\mu}$ -step
 - 11: $\text{diag}(\boldsymbol{\Sigma}) \leftarrow \frac{\frac{1}{|\mathcal{S}|} \sum_{i \in \mathcal{S}} \sum_k z_{i,k} (\mathbf{f}_i - \boldsymbol{\mu}_k)^2 + \frac{1}{|\mathcal{Q}|} \sum_{i \in \mathcal{Q}} \sum_k z_{i,k} (\mathbf{f}_i - \boldsymbol{\mu}_k)^2}{\gamma + 1}$ ▷ (3) $\boldsymbol{\Sigma}$ -step
 - 12: **end while**
 - 13: **return** \mathbf{z} ▷ Prediction with assignment variables
-

B Further details on TransCLIP implementation

This section aims to provide an additional pseudo-algorithm to supplement Section 3 as well as more details on TransCLIP hyper-parameters presented in Section 4. Our code is available at <https://github.com/MaxZanella/transduction-for-vlms> and a pseudo-code in Algorithm 1 that summarizes the main steps of the TransCLIP algorithm.

⁸For the zero-shot setting, we use the embedding of top-8 most confident initial predictions for each class as explained in Section 4.

Hardware. All our experiments were conducted on a single A100-40 GB. In terms of memory, TransCLIP consumes 16.9 GB when inferring on ImageNet, and can therefore process large datasets on a smaller 24 GB GPU.

Hyper-parameters. In practice, TransCLIP performs 10 iterations of \mathbf{z} , $\boldsymbol{\mu}$, $\boldsymbol{\Sigma}$ block-wise updates. For each \mathbf{z} -update, we perform 5 iterations, as we found it sufficient for convergence. In the zero-shot setting, we set $\lambda = 1$ and $\gamma = 0$ (as there are no support samples). In the few-shot setting, we set $\lambda = 0.5$ and search for the value of γ in $\{0.002, 0.01, 0.02, 0.2\}$. The number of validation shots is set at $\min(4, \#\text{shots})$, and we build a 1-nearest neighbor classifier with the query samples and their final class assignment to predict the class of each validation sample.

Prompt templates. We employ the prompt templates detailed in Table 23a for all our experiments in zero-shot setting unless otherwise explicitly specified. Only when specified, we utilize the custom template ensembling for ImageNet as in [69]. These templates are specified in Table 23b.

C Additional results.

We provide detailed results for all the studied vision backbones of CLIP over the 11 datasets to support the transferability of TransCLIP across both convolutional networks and transformer-based models. We additionally report other methods that do not fit into the transductive setting.

C.1 Zero-shot

In Table 8. We report performances of 5 CLIP encoders as well as the 8 billion parameter EVA-CLIP [54]. We compare TransCLIP-ZS to unsupervised methods namely TPT [42], MTA [67], SwapPrompt [40], and UPL [25]. Note that TPT and MTA are two test-time augmentation methods working on a single image at a time, thus they differ from our transductive setting, still we report their performance for informational purposes. As mentioned in Section 4, we slightly modified UPL to apply it to the test set in a transductive manner (transductive UPL is denoted UPL*). For fairness, we reevaluate the number of pseudo-labels to select and still found that 16 per class yields the best results on average, as seen in Table 22.

C.2 TransCLIP-ZS on top of few-shot methods

In Tables 9, 10, 11, 12 and 13. We report the performance of TransCLIP-ZS on top of CoOp [72], Tip-Adapter-F [69], PLOT [8], TaskRes [65] and ProGrad [73] for five encoders. The results are consistent with the main findings of Section 4 and indicate their generalization for several encoder architectures.

C.3 Cross-Dataset transferability

In Table 14. We report the performance of TransCLIP-ZS on top of CoOp [72], CoCoOp [71], ProGrad [73], PromptSRC [30] and MaPLE[29]. We additionally report PromptAlign [1], which is working on a single image at a time and thus differs from our transductive setting. Note that PromptSRC and MaPLE introduce learnable vision tokens, and are therefore not compatible with convolutional-based encoders. The results are similar to those of Section 4.

C.4 Domain Generalization

In Tables 15 and 16. We extend the results from Table 3 to five encoders. These results support those of Section 4 and show that TransCLIP can improve both zero- and few-shot model generalization for various encoders.

C.5 Transductive few-shot learning

In Tables 17, 18, 19, 20 and 21, we implemented transductive methods from the traditional few-shot literature that align the most with our work in terms of computational efficiency and wide applicability: TIM [5], LaplacianShot [75], BD-CSPN [36], TF [13], and PT-MAP [24]. Additionally,

due to the lack of transductive methods in Vision-Language and to ensure more comprehensive comparisons, we introduce a hybrid method named CoOp+UPL. This method combines prompt learning with both labeled shots and selected pseudo-labels following the methodology of UPL [25]. More details on each method and their validation procedure are outlined below. Methods with tunable hyper-parameters are fine-tuned using the validation split provided with each dataset. In line with other work [47], validation is performed for each dataset and for every shot number, setting the number of validation shots at $\min(4, \text{\#shots})$. Hyper-parameters are then optimized through a grid search to maximize accuracy on the validation set. Note that we only search for γ across 4 values for TransCLIP. More details on the grid search for each method is given below. Detailed results for the five architectures studied in this paper are available in Table 17, 18, 19, 20, 21. Now we describe the implementation details for each reported transductive few-shot methods.

Transductive Fine-Tuning. We follow the original implementation of Transductive Fine-Tuning [13]. The authors kept the hyper-parameters fixed for all datasets since the goal was to propose a simple baseline, with a temperature set to 1 and the number of training steps to 25. However, they pointed out possible improvements if the hyper-parameters were tuned for each dataset. Therefore, we search for the optimal temperature value by validation in $\{0.25, 0.5, 1, 2, 4\}$ and the number of iterations in $\{10, 15, 20, 25, 30, 35, 40\}$.

BD-CSPN. We follow the original implementation of BD-CSPN [36]. Regarding the hyper-parameters, this method generates Z pseudo-labels per class from the query set to augment the support set and to build the K prototype vectors. They also introduce a temperature scaling parameter ε for the computation of the prototype vectors. The authors set Z to 8 and the temperature scaling ε to 10. We search for the value of Z in $\{0, 1, 2, 3, 4, 5, 6, 7, 8, 9, 10\}$ and ε in $\{2.5, 5, 10, 20, 40\}$ by validation.

LaplacianShot. We follow the original implementation of LaplacianShot [75]. They balanced the Laplacian regularization term with a factor λ and used k -nearest neighbors consistency. We follow the proposed ranges to find the hyper-parameter values by validation, with λ in $\{0.1, 0.3, 0.5, 0.7, 0.8, 1, 1.2, 1.5\}$ and the number of neighbors to consider k in $\{3, 5, 10\}$.

PT-MAP. We follow the original implementation of PT-MAP [24]. In their work, the authors show a small performance sensitivity to the learning rate α used to update the class prototypes through iterative adaptation. Following their discussion, we search α in $\{0.2, 0.4\}$.

TIM. We follow the original implementation of TIM [5]. The authors proposed two solvers to find the solution to the minimization problem: gradient-descent TIM (TIM-GD) and alternating-direction method (TIM-ADM). We decide to focus on the second approach since there are fewer hyper-parameters to tune. They set the weighting factors of the cross-entropy, the marginal entropy, and the conditional entropy terms to 0.1, 1 and 0.1, respectively. They also introduced a temperature parameter τ in their classifier and set it to 15. We search for the values of the cross-entropy and the conditional entropy factors in $\{0.05, 0.1, 0.4, 0.7, 1\}$ and the temperature in $\{5, 10, 15, 30, 60\}$ by validation.

CoOp+UPL. We implement a natural extension of CoOp to include the pseudo-labels proposed by UPL. As in UPL, $N = 16$ hard pseudo-labels per class are generated according to the prediction’s confidence. Pseudo-labels from the query set $\mathcal{P} \subseteq \mathcal{Q}$ and labeled shots from \mathcal{S} are unified into a single learning set $\mathcal{S} \cup \mathcal{P}$. To separate the contribution of the pseudo-labels from the labeled shots, we split the cross-entropy loss function into two terms:

$$\begin{aligned} \mathcal{L}_{\mathcal{S} \cup \mathcal{P}}(\bar{\mathbf{V}}|\{\mathbf{x}_i\}_{i=1}^{|\mathcal{S} \cup \mathcal{P}|}) &= \beta \frac{1}{|\mathcal{S}|} \sum_{j \in \mathcal{S}} \mathcal{L}_{\text{CoOp}}(\bar{\mathbf{V}}|\mathbf{x}_j) \\ &+ (1 - \beta) \frac{1}{|\mathcal{P}|} \sum_{j \in \mathcal{P}} \mathcal{L}_{\text{UPL}}(\bar{\mathbf{V}}|\mathbf{x}_j), \quad \beta \in [0, 1] \end{aligned} \quad (8)$$

Where $\bar{\mathbf{V}}$ denotes the vector of learnable context token embeddings. Despite increased computational needs, we search for the value of β in $\{0.1, 0.3, 0.5, 0.7, 0.9\}$ by validation for the sake of fairness. The number of epochs, the learning rate and its schedule, the optimizer and the context tokens initialization follow exactly the CoOp implementation.

D Limitations

As discussed in Section 4, the gain of TransCLIP-ZS on top of few-shot methods tends to decrease when the number of shots is high (e.g., 16 shots) and future works may investigate this aspect.

Secondly, as TransCLIP’s performance relies greatly on its text-regularization term, TransCLIP is subject to some biases. One notable bias pertains to the quality of text embeddings within each class. Recent literature has highlighted that these embeddings exhibit a preference for more frequently occurring concepts [56]. However, this issue may be mitigated through our proposed few-shot extension (e.g., introducing labels for more challenging classes).

Table 8: Adaptation of CLIP on 11 classification datasets with zero-shot methods.

Method	ImageNet	SUN397	Aircraft	EuroSAT	StanfordCars	Food101	Pets	Flower102	Caltech101	DTD	UCF101	Average
CLIP-ResNet-50	58.0	58.8	17.0	36.2	55.7	77.4	85.8	66.0	85.7	42.9	61.9	58.7
+ TransCLIP-ZS	60.8_{+2.8}	64.2_{+5.4}	16.6 _{-0.4}	59.6_{+23.4}	57.9_{+2.2}	78.0_{+0.6}	89.3_{+3.6}	72.2_{+6.2}	88.6_{+3.0}	47.8_{+5.0}	68.8_{+6.9}	64.0_{+5.3}
TPT w/ a photo of a UPL*	60.7	61.5	17.6	28.3	58.5	74.9	84.5	62.7	87.0	40.8	60.8	57.9
SwapPrompt	61.6	63.3	16.7	52.1	63.1	78.0	89.1	69.3	85.7	47.0	65.8	62.9
	61.8	63.9	18.0	46.6	59.6	75.1	89.1	70.22	89.9	47.3	65.7	62.5
CLIP-ResNet-101	60.6	59.0	17.9	32.7	63.2	80.7	87.0	64.4	89.9	37.2	61.1	59.4
+ TransCLIP-ZS	64.8_{+4.2}	65.1_{+6.0}	19.2_{+1.3}	59.3_{+26.6}	68.6_{+5.4}	81.9_{+1.2}	89.8_{+2.7}	72.0_{+8.2}	93.0_{+3.1}	42.9_{+5.7}	68.9_{+7.8}	66.0_{+6.6}
UPL*	63.7	63.5	18.1	61.3	69.5	80.9	90.0	67.3	88.3	42.8	67.3	64.8
CLIP-ViT-B/32	61.9	62.1	19.1	45.2	60.2	80.4	87.4	66.5	91.5	42.7	63.6	61.9
+ TransCLIP-ZS	64.9_{+3.0}	67.6_{+5.5}	20.3_{+1.3}	59.0_{+13.8}	63.3_{+3.2}	81.5_{+1.1}	89.0_{+1.7}	74.4_{+7.9}	91.8_{+0.3}	50.4_{+7.7}	68.7_{+5.1}	66.5_{+4.6}
UPL*	64.6	66.4	19.1	59.3	64.8	81.0	89.8	69.7	89.8	48.3	67.8	65.5
CLIP-ViT-B/16	66.6	62.5	24.7	48.3	65.6	85.9	89.1	70.7	93.2	43.5	67.5	65.3
+ TransCLIP-ZS	70.3_{+3.7}	68.9_{+6.3}	26.9_{+2.2}	65.1_{+16.8}	69.4_{+3.8}	87.1_{+1.2}	92.6_{+3.5}	76.7_{+5.9}	92.7_{-0.5}	49.5_{+6.0}	74.4_{+6.9}	70.3_{+5.1}
TPT w/ a photo of a MTA w/ a photo of a UPL*	69.0	65.5	24.8	42.4	66.9	84.7	87.8	69.0	94.2	47.8	68.0	65.5
	69.3	65.0	25.3	38.7	68.1	85.0	88.2	68.3	94.1	45.6	68.1	65.1
	69.6	67.4	24.7	69.5	71.1	85.8	92.4	73.5	91.9	47.7	73.7	69.8
CLIP-ViT-L/14	72.9	67.7	32.6	60.3	76.9	90.9	93.5	79.5	95.2	53.5	74.9	72.5
+ TransCLIP-ZS	77.2_{+4.3}	73.5_{+5.9}	35.3_{+2.7}	75.9_{+15.6}	79.0_{+2.1}	91.9_{+1.0}	94.7_{+1.2}	85.3_{+5.8}	97.4_{+2.3}	60.0_{+6.5}	81.7_{+6.7}	77.4_{+4.9}
UPL*	76.6	72.2	35.1	61.7	82.6	90.9	95.2	83.7	94.9	57.2	80.1	75.5
EVA-CLIP-8B	82.5	76.4	57.9	62.5	94.8	93.5	96.3	86.8	98.0	63.6	84.4	81.5
+ TransCLIP-ZS	84.6_{+2.1}	80.1_{+3.7}	59.4_{+1.5}	81.9_{+19.4}	95.0_{+0.2}	93.9_{+0.4}	96.3_{+0.0}	91.8_{+5.0}	98.3_{+0.3}	68.6_{+5.0}	93.6_{+9.2}	85.8_{+4.3}

Table 9: TransCLIP atop inductive vision-language zero-shot and popular few-shot methods for ResNet-50 vision encoder.

Method	ImageNet	SUN397	Aircraft	EuroSAT	StanfordCars	Food101	Pets	Flower102	Caltech101	DTD	UCF101	Average
0-shot												
CLIP-ResNet-50	58.0	58.8	17.0	36.2	55.7	77.4	85.8	66.0	85.7	42.9	61.9	58.7
+ TransCLIP-ZS	60.8_{+2.8}	64.2_{+5.4}	16.6 _{-0.4}	59.6_{+23.4}	57.9_{+2.2}	78.0_{+0.6}	89.3_{+3.6}	72.2_{+6.2}	88.6_{+3.0}	47.8_{+5.0}	68.8_{+6.9}	64.0_{+5.3}
1-shot												
CoOp	57.4	60.0	8.5	49.4	55.8	74.2	85.9	69.0	87.3	45.1	62.9	59.6
+ TransCLIP-ZS	60.2_{+2.8}	65.3_{+5.3}	9.3_{+0.8}	57.1_{+7.7}	58.8_{+3.0}	77.0_{+2.7}	86.9_{+1.1}	81.6_{+12.6}	88.7_{+1.4}	53.2_{+8.2}	69.1_{+6.1}	64.3_{+4.7}
TIP-Adapter-F	61.1	62.1	18.6	50.2	59.2	77.1	86.3	78.1	88.3	47.6	64.7	63.0
+ TransCLIP-ZS	62.3_{+1.1}	66.5_{+4.3}	19.2_{+0.6}	66.4_{+16.2}	60.3_{+1.1}	77.8_{+0.7}	89.2_{+2.9}	89.1_{+11.0}	88.9_{+0.6}	52.8_{+5.2}	71.0_{+6.3}	67.6_{+4.6}
TaskRes	61.4	62.0	20.9	59.8	59.4	74.8	84.4	75.4	88.5	49.6	64.5	63.7
+ TransCLIP-ZS	62.4_{+1.0}	66.4_{+4.4}	20.4 _{-0.5}	69.4_{+9.6}	60.2_{+0.9}	77.1_{+2.3}	87.1_{+2.7}	84.4_{+9.0}	88.3_{-0.3}	56.8_{+7.2}	69.3_{+4.8}	67.4_{+3.7}
ProGrad	57.8	60.9	18.9	55.0	58.6	76.3	88.0	72.2	88.1	46.4	64.1	62.4
+ TransCLIP-ZS	60.5_{+2.7}	66.0_{+5.1}	18.4 _{-0.6}	69.4_{+14.4}	60.5_{+1.9}	77.7_{+1.3}	87.9_{-0.0}	83.8_{+11.6}	88.7_{+0.6}	51.8_{+5.4}	71.8_{+7.7}	67.0_{+4.6}
4-shot												
CoOp	59.8	63.5	20.5	71.3	62.9	73.8	87.0	85.7	89.3	54.0	67.6	66.8
+ TransCLIP-ZS	61.7_{+1.9}	68.1_{+4.6}	21.8_{+1.3}	74.4_{+3.1}	64.0_{+1.1}	76.9_{+3.1}	88.9_{+1.9}	91.4_{+5.8}	90.5_{+1.3}	59.6_{+5.7}	73.8_{+6.3}	70.1_{+3.3}
TIP-Adapter-F	62.6	65.6	25.4	70.5	63.4	77.9	86.7	87.5	91.1	55.4	70.9	68.8
+ TransCLIP-ZS	63.0_{+0.4}	68.5_{+2.9}	24.6 _{-0.7}	70.9_{+0.4}	63.2 _{-0.2}	78.1_{+0.2}	89.0_{+2.4}	92.4_{+4.9}	90.3_{-0.8}	59.7_{+4.3}	76.7_{+5.8}	70.6_{+1.8}
TaskRes	62.8	66.7	23.1	70.3	66.3	76.8	86.7	79.3	90.6	57.4	67.9	68.0
+ TransCLIP-ZS	63.3_{+0.5}	69.2_{+2.5}	21.7 _{-1.5}	72.2_{+1.9}	64.5 _{-1.8}	77.9_{+1.2}	88.9_{+2.2}	85.1_{+5.8}	90.4_{-0.1}	60.9_{+3.5}	74.4_{+6.5}	69.9_{+1.9}
ProGrad	62.5	69.3	23.1	74.1	65.1	77.7	89.6	91.7	90.8	59.8	76.2	70.9
+ TransCLIP-ZS	62.5_{+1.2}	69.3_{+3.3}	23.1 _{-0.4}	74.1_{+3.6}	65.1 _{-0.3}	77.7_{+1.8}	89.6_{+1.2}	91.7_{+7.4}	90.8_{+1.0}	59.8_{+5.3}	76.2_{+7.4}	70.9_{+2.9}
16-shot												
CoOp	63.0	69.4	31.4	82.2	73.6	74.5	86.6	94.6	91.8	63.3	74.4	73.2
+ TransCLIP-ZS	63.5_{+0.5}	71.1_{+1.7}	29.9 _{-1.5}	81.3_{-0.8}	70.5 _{-3.1}	77.5_{+2.9}	88.6_{+2.0}	94.9_{+0.3}	91.4_{-0.5}	65.7_{+2.4}	79.4_{+5.0}	74.0_{+0.8}
TIP-Adapter-F	65.2	71.2	33.9	83.3	74.3	78.9	89.0	92.7	92.5	66.0	76.5	74.9
+ TransCLIP-ZS	64.6_{-0.5}	71.0_{-0.2}	33.3_{-0.7}	80.5_{-2.8}	72.9 _{-1.5}	78.4_{-0.5}	89.4_{-0.5}	94.1_{+1.4}	91.0_{-1.6}	65.5_{-0.6}	79.9_{+3.4}	74.6_{-0.3}
TaskRes	64.4	70.8	29.1	75.5	69.8	78.6	89.3	94.7	90.5	64.7	79.4	73.3
+ TransCLIP-ZS	64.4_{-0.2}	70.8_{-0.6}	29.1 _{-3.9}	75.5_{-4.2}	69.8 _{-5.0}	78.6_{-0.1}	89.3_{-0.8}	94.7_{+0.3}	90.5_{-2.5}	64.7_{-2.6}	79.4_{+3.6}	73.3_{-1.2}
ProGrad	63.4	69.9	31.8	81.9	73.9	77.0	88.2	94.2	92.3	63.6	75.4	73.8
+ TransCLIP-ZS	63.5_{+0.2}	71.2_{+1.3}	29.0 _{-2.8}	79.8_{-2.2}	70.2 _{-3.7}	78.4_{+1.4}	89.2_{+1.0}	94.5_{+0.3}	91.0_{-1.3}	65.7_{+2.0}	79.9_{+4.5}	73.9_{+0.1}

Table 10: TransCLIP atop inductive vision-language zero-shot and popular few-shot methods for ResNet-101 vision encoder.

Method	ImageNet	SUN397	Aircraft	EuroSAT	StanfordCars	Food101	Pets	Flower102	Caltech101	DTD	UCF101	Average
0-shot												
CLIP-ResNet-101	60.6	59.0	17.9	32.7	63.2	80.7	87.0	64.4	89.9	37.2	61.1	59.4
+ TransCLIP-ZS	64.8 _{+4.2}	65.1 _{+6.0}	19.2 _{+1.3}	59.3 _{+26.6}	68.6 _{+5.4}	81.9 _{+1.2}	89.8 _{+2.7}	72.6 _{+8.2}	93.0 _{+3.1}	42.9 _{+5.7}	68.9 _{+7.8}	66.0 _{+6.6}
1-shot												
CoOp	60.8	61.3	14.8	51.0	64.5	76.9	86.5	69.5	89.8	44.3	65.7	62.3
+ TransCLIP-ZS	64.3 _{+3.5}	66.3 _{+4.9}	16.3 _{+1.6}	58.2 _{+7.2}	70.2 _{+5.7}	79.8 _{+2.9}	89.1 _{+2.6}	80.6 _{+11.1}	92.5 _{+2.8}	49.9 _{+5.5}	72.7 _{+6.9}	67.3 _{+5.0}
TIP-Adapter-F	63.6	61.4	19.2	46.3	64.8	80.2	87.2	77.5	91.7	46.3	65.9	64.0
+ TransCLIP-ZS	66.4 _{+2.8}	67.1 _{+5.7}	21.0 _{+1.8}	66.1 _{+19.8}	70.6 _{+5.7}	81.8 _{+1.6}	90.3 _{+3.1}	88.4 _{+10.9}	92.8 _{+1.1}	51.7 _{+5.4}	73.1 _{+7.3}	69.9 _{+5.9}
TaskRes	63.6	62.6	22.5	52.9	66.4	78.2	86.3	74.8	91.2	49.2	67.3	65.0
+ TransCLIP-ZS	66.6 _{+3.0}	67.9 _{+5.3}	23.3 _{+0.8}	64.0 _{+11.1}	70.3 _{+3.9}	80.7 _{+2.4}	89.7 _{+3.3}	85.4 _{+10.6}	92.1 _{+0.8}	53.5 _{+4.3}	74.2 _{+6.9}	69.8 _{+4.8}
4-shot												
CoOp	63.0	65.9	26.8	67.4	70.3	77.8	87.4	85.5	92.3	55.5	72.3	69.5
+ TransCLIP-ZS	66.0 _{+3.0}	69.7 _{+3.8}	27.7 _{+1.0}	71.4 _{+4.1}	73.8 _{+3.5}	80.5 _{+2.7}	90.1 _{+2.7}	91.4 _{+5.8}	93.8 _{+1.5}	59.7 _{+4.1}	77.3 _{+4.9}	72.9 _{+3.4}
TIP-Adapter-F	65.0	65.3	27.4	68.6	70.9	81.2	88.4	90.1	93.0	58.3	74.1	71.1
+ TransCLIP-ZS	67.4 _{+2.4}	69.8 _{+4.4}	28.6 _{+1.1}	70.8 _{+2.2}	74.0 _{+3.1}	82.2 _{+1.0}	90.6 _{+2.2}	93.5 _{+3.3}	93.6 _{+0.6}	62.0 _{+3.7}	79.2 _{+5.1}	73.8 _{+2.7}
TaskRes	65.3	68.0	24.3	61.9	72.4	80.4	88.0	78.6	92.9	56.5	71.0	69.0
+ TransCLIP-ZS	67.7 _{+2.4}	71.3 _{+3.3}	25.4 _{+1.1}	68.5 _{+6.5}	74.9 _{+2.5}	81.8 _{+1.4}	90.9 _{+2.8}	86.9 _{+8.3}	93.8 _{+0.9}	61.6 _{+5.2}	78.5 _{+7.5}	72.8 _{+3.8}
16-shot												
CoOp	66.5	71.0	34.8	83.4	79.1	78.9	89.0	95.1	93.5	65.1	78.1	75.9
+ TransCLIP-ZS	68.5 _{+2.0}	73.0 _{+2.0}	34.9 _{+0.1}	83.0 _{-0.4}	79.8 _{+0.8}	81.1 _{+2.3}	90.9 _{+1.9}	95.8 _{+0.7}	93.6 _{+0.1}	68.2 _{+3.1}	81.2 _{+3.1}	77.3 _{+1.4}
TIP-Adapter-F	68.3	72.8	36.2	82.0	80.5	81.9	89.9	94.4	93.9	67.6	79.4	77.0
+ TransCLIP-ZS	69.2 _{+0.9}	73.5 _{+0.7}	36.6 _{+0.4}	80.0 _{-2.0}	81.3 _{+0.8}	82.4 _{+0.5}	91.7 _{+1.8}	95.3 _{+0.9}	94.2 _{+0.3}	68.0 _{+0.3}	81.9 _{+2.6}	77.7 _{+0.7}
TaskRes	67.6	72.1	35.5	74.9	80.6	81.9	89.5	94.9	94.6	68.1	79.5	76.3
+ TransCLIP-ZS	69.3 _{+1.7}	73.3 _{+1.2}	34.8 _{-0.8}	73.9 _{-1.0}	80.8 _{+0.2}	82.6 _{+0.7}	90.9 _{+1.4}	95.5 _{+0.6}	94.5 _{-0.1}	68.3 _{+0.2}	82.8 _{+3.3}	77.0 _{+0.7}

Table 11: TransCLIP atop inductive vision-language zero-shot and popular few-shot methods for ViT-B/32 vision encoder.

Method	ImageNet	SUN397	Aircraft	EuroSAT	StanfordCars	Food101	Pets	Flower102	Caltech101	DTD	UCF101	Average
0-shot												
CLIP-ViT-B/32	61.9	62.1	19.1	45.2	60.2	80.4	87.4	66.5	91.5	42.7	63.6	61.9
+ TransCLIP-ZS	64.9 _{+3.0}	67.6 _{+5.5}	20.3 _{+1.3}	59.0 _{+13.8}	63.3 _{+3.2}	81.5 _{+1.1}	89.0 _{+1.7}	74.4 _{+7.9}	91.8 _{+0.3}	50.4 _{+7.7}	68.7 _{+5.1}	66.5 _{+4.6}
1-shot												
CoOp	60.8	63.3	15.6	51.9	59.5	75.7	87.7	71.5	91.8	47.1	66.0	62.8
+ TransCLIP-ZS	63.9 _{+3.1}	68.3 _{+5.0}	17.7 _{+2.0}	64.9 _{+13.0}	63.4 _{+3.9}	78.8 _{+3.0}	89.2 _{+1.5}	84.3 _{+12.8}	92.2 _{+0.4}	53.1 _{+5.9}	71.9 _{+5.9}	68.0 _{+5.1}
TIP-Adapter-F	64.3	65.4	22.2	59.7	61.1	80.4	87.5	81.1	92.4	50.9	66.5	66.5
+ TransCLIP-ZS	66.5 _{+2.1}	69.9 _{+4.5}	23.3 _{+1.1}	71.8 _{+12.1}	64.8 _{+3.7}	81.4 _{+1.0}	89.5 _{+1.9}	89.6 _{+8.5}	92.3 _{-0.2}	55.9 _{+5.0}	72.5 _{+5.9}	70.7 _{+4.1}
TaskRes	64.6	65.3	23.8	60.8	62.4	79.0	84.6	77.7	91.2	52.7	67.5	66.3
+ TransCLIP-ZS	66.7 _{+2.1}	69.8 _{+4.5}	23.9 _{+0.1}	73.4 _{+12.6}	64.2 _{+1.8}	80.7 _{+1.7}	88.2 _{+3.5}	86.6 _{+8.9}	91.8 _{+0.5}	57.0 _{+4.3}	72.8 _{+5.3}	70.5 _{+4.1}
ProGrad	62.0	64.8	21.1	53.5	60.5	78.2	87.9	74.4	91.5	51.1	66.6	64.7
+ TransCLIP-ZS	64.9 _{+2.9}	69.2 _{+4.4}	22.2 _{+1.1}	63.3 _{+9.8}	63.6 _{+3.1}	80.2 _{+2.0}	89.6 _{+1.7}	86.4 _{+12.0}	92.1 _{+0.6}	55.8 _{+4.7}	72.0 _{+5.4}	69.0 _{+4.3}
4-shot												
CoOp	63.2	67.1	24.1	67.8	66.4	75.5	88.8	87.6	92.9	55.1	74.9	69.4
+ TransCLIP-ZS	65.7 _{+2.6}	70.7 _{+3.7}	25.3 _{+1.3}	77.2 _{+9.4}	69.4 _{+3.0}	78.8 _{+3.3}	90.5 _{+1.7}	92.0 _{+4.4}	93.4 _{+0.5}	59.3 _{+4.2}	79.3 _{+4.4}	72.9 _{+3.5}
TIP-Adapter-F	65.8	68.3	28.8	71.5	67.6	80.9	88.6	88.9	94.6	58.0	75.1	71.6
+ TransCLIP-ZS	67.5 _{+1.7}	72.0 _{+3.7}	28.5 _{-0.3}	76.8 _{+5.3}	68.5 _{+0.9}	81.7 _{+0.8}	90.2 _{+1.6}	92.5 _{+3.5}	93.8 _{-0.8}	62.1 _{+4.1}	78.5 _{+3.5}	73.8 _{+2.2}
TaskRes	66.1	70.1	25.3	68.8	69.5	80.4	87.3	81.8	93.9	57.9	71.7	70.2
+ TransCLIP-ZS	67.8 _{+1.7}	72.7 _{+2.6}	25.6 _{+0.4}	77.1 _{+8.3}	70.3 _{+0.8}	81.6 _{+1.1}	90.0 _{+2.7}	88.3 _{+6.5}	94.2 _{+0.3}	61.9 _{+4.0}	76.1 _{+4.4}	73.2 _{+3.0}
ProGrad	65.2	69.6	24.8	63.0	66.5	79.2	89.4	87.7	93.4	56.1	73.7	69.9
+ TransCLIP-ZS	67.1 _{+1.9}	72.7 _{+3.0}	25.6 _{+0.8}	74.0 _{+11.0}	69.5 _{+2.9}	80.9 _{+1.7}	91.1 _{+1.7}	92.7 _{+5.0}	92.8 _{-0.5}	61.2 _{+5.1}	78.0 _{+4.3}	73.2 _{+3.4}
16-shot												
CoOp	66.8	72.3	32.8	82.4	76.1	78.6	88.8	95.5	94.9	64.9	78.5	75.6
+ TransCLIP-ZS	68.4 _{+1.6}	74.2 _{+1.9}	32.7 _{-0.1}	84.0 _{+1.6}	77.1 _{+1.0}	80.7 _{+2.2}	90.2 _{+1.4}	95.5 _{-0.0}	95.4 _{+0.5}	67.3 _{+2.4}	81.2 _{+2.7}	77.0 _{+1.4}
TIP-Adapter-F	68.4	74.1	34.8	83.4	77.0	81.7	90.4	94.3	95.1	68.0	80.5	77.1
+ TransCLIP-ZS	69.0 _{+0.5}	74.8 _{+0.7}	35.0 _{+0.2}	84.1 _{+0.7}	77.3 _{+0.3}	82.0 _{+0.3}	91.0 _{+0.6}	95.3 _{+1.0}	95.1 _{-0.1}	67.4 _{-0.6}	82.5 _{+2.0}	77.6 _{+0.5}
TaskRes	68.2	73.5	37.0	76.9	78.1	81.4	89.4	95.5	95.6	68.1	80.3	76.7
+ TransCLIP-ZS	69.2 _{+1.1}	74.6 _{+1.0}	35.3 _{-1.7}	80.3 _{+3.4}	77.2 _{-0.8}	82.0 _{+0.6}	90.7 _{+1.3}	95.1 _{-0.4}	94.8 _{-0.9}	67.8 _{-0.4}	82.3 _{+2.0}	77.2 _{+0.5}
ProGrad	66.9	73.2	33.2	80.6	76.2	80.2	89.4	95.1	95.0	65.3	80.0	75.9
+ TransCLIP-ZS	68.4 _{+1.5}	74.8 _{+1.5}	33.2 _{-0.0}	82.8 _{+2.2}	77.1 _{+0.9}	81.6 _{+1.4}	90.4 _{+1.0}	95.3 _{+0.3}	94.3 _{-0.8}	67.8 _{+2.5}	82.7 _{+2.8}	77.1 _{+1.2}

Table 12: TransCLIP atop inductive vision-language zero-shot and popular few-shot methods for ViT-B/16 vision encoder.

Method	ImageNet	SUN397	Aircraft	EuroSAT	StanfordCars	Food101	Pets	Flower102	Cats101	DTD	UCF101	Average
0-shot												
CLIP-ViT-B/16	66.6	62.5	24.7	48.3	65.6	85.9	89.1	70.7	93.2	43.5	67.5	65.3
+ TransCLIP-ZS	70.3 _{+3.7}	68.9 _{+6.3}	26.9 _{+2.2}	65.1 _{+16.8}	69.4 _{+3.8}	87.1 _{+11.2}	92.6 _{+3.5}	76.7 _{+5.9}	92.7 _{-0.5}	49.5 _{+6.0}	74.4 _{+6.9}	70.3 _{+5.1}
CoOp	65.7	66.9	20.7	56.4	67.6	84.3	90.2	78.2	92.5	50.1	71.2	67.6
+ TransCLIP-ZS	69.3 _{+3.6}	71.5 _{+4.6}	23.8 _{+3.1}	65.3 _{+8.9}	71.9 _{+4.3}	86.3 _{+2.0}	91.9 _{+1.8}	89.8 _{+11.5}	93.8 _{+1.3}	55.4 _{+5.4}	77.7 _{+6.5}	72.4 _{+4.8}
TIP-Adapter-F	69.5	67.2	28.8	67.8	67.1	85.8	90.6	83.7	94.0	51.6	73.4	70.9
+ TransCLIP-ZS	72.0 _{+2.5}	71.8 _{+4.6}	30.7 _{+1.9}	76.9 _{+9.1}	71.0 _{+3.9}	86.9 _{+1.1}	93.1 _{+2.4}	92.8 _{+9.1}	93.5 _{-0.5}	57.7 _{+6.1}	80.0 _{+6.7}	75.1 _{+4.3}
PLOT	66.9	67.0	28.9	72.8	68.5	84.9	91.9	81.8	94.0	52.8	74.7	71.0
+ TransCLIP-ZS	75.8 _{+8.9}	70.3 _{+3.3}	28.1 _{-0.8}	78.8 _{+6.0}	70.0 _{+1.6}	85.3 _{+0.4}	91.1 _{-0.8}	93.2 _{+11.4}	94.0 _{-0.0}	56.7 _{+3.9}	81.4 _{+6.7}	75.3 _{+3.7}
TaskRes	69.6	68.1	31.2	65.6	69.1	84.5	90.2	81.6	93.6	53.4	71.8	70.8
+ TransCLIP-ZS	72.0 _{+2.5}	72.5 _{+4.4}	31.4 _{+0.2}	73.7 _{+8.1}	71.6 _{+2.4}	86.5 _{+2.0}	91.6 _{+1.5}	90.7 _{+9.1}	94.0 _{+0.4}	59.4 _{+6.0}	76.4 _{+4.6}	74.5 _{+3.7}
ProGrad	67.0	67.0	28.7	57.0	68.2	84.9	91.4	80.8	93.5	52.8	73.3	69.5
+ TransCLIP-ZS	70.1 _{+3.1}	71.6 _{+4.6}	30.5 _{+1.8}	70.9 _{+13.9}	72.3 _{+4.1}	86.5 _{+1.6}	92.7 _{+1.4}	91.5 _{+10.7}	94.1 _{+0.7}	57.9 _{+5.1}	79.3 _{+6.1}	74.3 _{+4.8}
1-shot												
CoOp	68.8	69.7	30.8	69.6	74.4	84.5	92.5	92.2	94.5	59.4	77.5	74.0
+ TransCLIP-ZS	71.4 _{+2.6}	73.3 _{+3.5}	33.1 _{+2.3}	77.2 _{+7.5}	77.7 _{+3.2}	86.5 _{+1.9}	93.6 _{+1.1}	95.3 _{+3.1}	95.1 _{+0.6}	63.0 _{+3.6}	81.8 _{+4.3}	77.1 _{+3.1}
TIP-Adapter-F	70.7	70.8	35.7	76.8	74.1	86.5	91.9	92.1	94.8	59.8	78.1	75.6
+ TransCLIP-ZS	72.7 _{+1.9}	74.4 _{+3.5}	36.1 _{+0.5}	79.7 _{+2.9}	75.9 _{+1.8}	87.4 _{+0.9}	93.2 _{+1.3}	95.5 _{+3.3}	95.1 _{+0.3}	64.0 _{+4.2}	83.3 _{+5.2}	77.9 _{+2.3}
PLOT	70.0	71.8	34.8	84.7	76.6	83.5	92.8	93.2	94.9	61.0	79.7	76.6
+ TransCLIP-ZS	77.2 _{+7.2}	73.5 _{+1.7}	33.9 _{-0.9}	81.8 _{-2.9}	75.8 _{-0.8}	85.6 _{+2.2}	92.5 _{-0.3}	95.8 _{+2.6}	94.8 _{-0.1}	63.6 _{+2.6}	83.3 _{+3.6}	78.0 _{+1.4}
TaskRes	71.0	72.8	33.3	73.8	76.1	86.1	91.9	85.0	94.9	59.7	75.5	74.6
+ TransCLIP-ZS	73.0 _{+2.0}	75.3 _{+2.5}	34.4 _{+1.1}	78.1 _{+4.4}	77.2 _{+1.1}	87.3 _{+1.2}	93.0 _{+1.1}	92.4 _{+7.4}	95.1 _{+0.2}	64.3 _{+4.6}	79.2 _{+3.7}	77.2 _{+2.7}
ProGrad	70.2	71.7	34.0	69.5	75.0	85.4	92.0	91.1	94.4	59.8	77.9	74.6
+ TransCLIP-ZS	72.3 _{+2.1}	75.0 _{+3.3}	35.5 _{+1.6}	74.9 _{+5.3}	77.9 _{+2.9}	87.0 _{+1.5}	93.7 _{+1.7}	95.3 _{+4.2}	95.1 _{+0.8}	64.8 _{+5.1}	83.2 _{+5.4}	77.7 _{+3.1}
4-shot												
CoOp	71.9	74.9	43.3	85.0	82.8	84.2	91.9	96.8	95.8	69.7	83.1	79.9
+ TransCLIP-ZS	73.3 _{+1.4}	76.6 _{+1.8}	42.9 _{-0.4}	86.0 _{+1.0}	83.0 _{+0.2}	86.3 _{+2.1}	93.2 _{+1.2}	97.5 _{+0.8}	95.9 _{+0.1}	71.3 _{+1.7}	85.4 _{+2.3}	81.1 _{+1.1}
TIP-Adapter-F	73.3	76.0	44.6	85.9	82.3	86.8	92.6	96.2	95.7	70.8	83.9	80.7
+ TransCLIP-ZS	74.2 _{+0.9}	76.8 _{+0.8}	44.9 _{+0.3}	85.2 _{-0.7}	82.7 _{+0.4}	87.4 _{+0.6}	93.5 _{+0.9}	96.9 _{+0.7}	95.7 _{-0.1}	69.2 _{-1.5}	85.6 _{+1.7}	81.1 _{+0.4}
PLOT	72.5	76.0	46.8	92.1	84.6	85.6	92.5	97.1	96.0	71.1	84.8	81.7
+ TransCLIP-ZS	77.8 _{+5.3}	75.0 _{-1.0}	41.8 _{-4.9}	84.6 _{-7.5}	79.6 _{-4.9}	85.9 _{+0.2}	92.2 _{-0.4}	97.3 _{+0.1}	95.0 _{-1.0}	68.7 _{-2.4}	85.7 _{+0.9}	80.3 _{-1.4}
TaskRes	73.0	76.0	44.8	80.7	83.5	86.9	92.5	97.3	95.9	70.9	83.4	80.5
+ TransCLIP-ZS	74.1 _{+1.0}	76.9 _{+0.8}	43.6 _{-1.2}	80.5 _{-0.3}	82.8 _{-0.7}	87.5 _{+0.6}	92.9 _{+0.4}	97.6 _{+0.3}	96.0 _{+0.1}	70.2 _{-0.7}	86.2 _{+2.8}	80.8 _{+0.3}
ProGrad	72.1	75.1	42.8	83.6	82.9	85.8	92.9	96.6	95.9	68.9	82.6	79.9
+ TransCLIP-ZS	73.5 _{+1.4}	76.8 _{+1.7}	42.8 _{-0.0}	83.7 _{+0.2}	83.1 _{+0.2}	87.2 _{+1.3}	93.7 _{+0.8}	97.4 _{+0.8}	96.0 _{+0.1}	71.4 _{+2.5}	86.1 _{+3.4}	81.1 _{+1.1}
16-shot												
CoOp	71.9	74.9	43.3	85.0	82.8	84.2	91.9	96.8	95.8	69.7	83.1	79.9
+ TransCLIP-ZS	73.3 _{+1.4}	76.6 _{+1.8}	42.9 _{-0.4}	86.0 _{+1.0}	83.0 _{+0.2}	86.3 _{+2.1}	93.2 _{+1.2}	97.5 _{+0.8}	95.9 _{+0.1}	71.3 _{+1.7}	85.4 _{+2.3}	81.1 _{+1.1}
TIP-Adapter-F	73.3	76.0	44.6	85.9	82.3	86.8	92.6	96.2	95.7	70.8	83.9	80.7
+ TransCLIP-ZS	74.2 _{+0.9}	76.8 _{+0.8}	44.9 _{+0.3}	85.2 _{-0.7}	82.7 _{+0.4}	87.4 _{+0.6}	93.5 _{+0.9}	96.9 _{+0.7}	95.7 _{-0.1}	69.2 _{-1.5}	85.6 _{+1.7}	81.1 _{+0.4}
PLOT	72.5	76.0	46.8	92.1	84.6	85.6	92.5	97.1	96.0	71.1	84.8	81.7
+ TransCLIP-ZS	77.8 _{+5.3}	75.0 _{-1.0}	41.8 _{-4.9}	84.6 _{-7.5}	79.6 _{-4.9}	85.9 _{+0.2}	92.2 _{-0.4}	97.3 _{+0.1}	95.0 _{-1.0}	68.7 _{-2.4}	85.7 _{+0.9}	80.3 _{-1.4}
TaskRes	73.0	76.0	44.8	80.7	83.5	86.9	92.5	97.3	95.9	70.9	83.4	80.5
+ TransCLIP-ZS	74.1 _{+1.0}	76.9 _{+0.8}	43.6 _{-1.2}	80.5 _{-0.3}	82.8 _{-0.7}	87.5 _{+0.6}	92.9 _{+0.4}	97.6 _{+0.3}	96.0 _{+0.1}	70.2 _{-0.7}	86.2 _{+2.8}	80.8 _{+0.3}
ProGrad	72.1	75.1	42.8	83.6	82.9	85.8	92.9	96.6	95.9	68.9	82.6	79.9
+ TransCLIP-ZS	73.5 _{+1.4}	76.8 _{+1.7}	42.8 _{-0.0}	83.7 _{+0.2}	83.1 _{+0.2}	87.2 _{+1.3}	93.7 _{+0.8}	97.4 _{+0.8}	96.0 _{+0.1}	71.4 _{+2.5}	86.1 _{+3.4}	81.1 _{+1.1}

Table 13: TransCLIP atop inductive vision-language zero-shot and popular few-shot methods for ViT-L/14 vision encoder.

Method	ImageNet	SUN397	Aircraft	EuroSAT	StanfordCars	Food101	Pets	Flower102	Cats101	DTD	UCF101	Average
0-shot												
CLIP-ViT-L/14	72.9	67.7	32.6	60.3	76.9	90.9	93.5	79.5	95.2	53.5	74.9	72.5
+ TransCLIP-ZS	77.2 _{+4.3}	73.5 _{+5.9}	35.3 _{+2.7}	75.9 _{+15.6}	79.0 _{+2.1}	91.9 _{+1.0}	94.7 _{+1.2}	85.3 _{+5.8}	97.4 _{+2.3}	60.0 _{+6.5}	81.7 _{+6.7}	77.4 _{+4.9}
CoOp	71.5	68.9	36.9	68.4	78.8	89.0	94.0	87.2	95.0	58.6	78.7	75.2
+ TransCLIP-ZS	75.9 _{+4.5}	74.3 _{+5.4}	38.0 _{+1.0}	80.4 _{+11.9}	81.5 _{+2.8}	91.0 _{+2.1}	95.3 _{+1.4}	95.0 _{+7.8}	96.3 _{+1.3}	64.1 _{+5.5}	83.5 _{+4.8}	79.6 _{+4.4}
TIP-Adapter-F	76.4	71.0	38.5	67.8	79.2	91.0	93.2	90.9	95.3	59.3	77.9	76.4
+ TransCLIP-ZS	78.8 _{+2.4}	75.5 _{+4.5}	40.9 _{+2.4}	75.5 _{+7.7}	80.5 _{+1.3}	91.9 _{+0.9}	94.1 _{+0.9}	97.4 _{+6.5}	96.9 _{+1.6}	64.9 _{+5.6}	83.8 _{+5.9}	80.0 _{+3.6}
TaskRes	76.2	71.4	39.6	71.8	79.9	89.8	93.5	87.4	95.0	60.1	77.7	76.6
+ TransCLIP-ZS	78.8 _{+2.5}	75.9 _{+4.5}	41.2 _{+1.6}	82.0 _{+10.2}	81.1 _{+1.2}	91.5 _{+1.6}	94.9 _{+1.4}	94.7 _{+7.2}	96.2 _{+1.2}	65.7 _{+5.6}	83.8 _{+6.1}	80.5 _{+3.9}
ProGrad	73.6	71.1	38.4	71.4	80.0	90.5	94.4	89.0	95.7	58.8	80.2	76.6
+ TransCLIP-ZS	76.9 _{+3.3}	75.8 _{+4.7}	41.1 _{+2.8}	78.7 _{+7.3}	81.1 _{+1.1}	91.7 _{+1.2}	95.6 _{+1.2}	97.5 _{+8.5}	96.4 _{+0.7}	65.9 _{+7.0}	84.0 _{+3.8}	80.4 _{+3.8}
1-shot												
CoOp	74.9	73.1	43.6	76.2	83.3	88.8	94.6	95.9	96.7	64.1	83.0	79.5
+ TransCLIP-ZS	77.9 _{+3.0}	76.9 _{+3.8}	44.0 _{+0.5}	81.6 _{+5.5}	84.0 _{+0.7}	91.2 _{+2.4}	95.8 _{+1.2}	97.3 _{+1.4}	97.4 _{+0.7}	67.7 _{+3.6}	85.9 _{+3.0}	81.8 _{+2.3}
TIP-Adapter-F	77.0	74.1	47.4	81.4	82.3	91.2	94.0	95.5	96.5	64.4	83.9	80.7
+ TransCLIP-ZS	79.0 _{+2.0}	77.2 _{+3.1}	47.6 _{+0.2}	83.0 _{+1.6}	82.9 _{+0.6}	91.9 _{+0.7}	94.8 _{+0.8}	98.5 _{+3.0}	97.5 _{+1.1}	69.0 _{+4.6}	87.7 _{+3.7}	82.6 _{+1.9}
TaskRes	77.1	74.9	42.5	77.3	83.6	90.6	94.4	90.1	96.6	65.1	80.0	79.3
+ TransCLIP-ZS	79.4 _{+2.2}	78.5 _{+3.6}	44.9 _{+2.4}	81.4 _{+4.1}	83.2 _{-0.3}	91.8 _{+1.1}	95.7 _{+1.3}	96.5 _{+6.4}	97.7 _{+1.1}	68.0 _{+2.9}	86.1 _{+6.1}	82.1 _{+2.8}
ProGrad	76.5	74.9	44.5	79.3	83.9	90.6	94.8	95.6	96.7	66.1	83.9	80.6
+ TransCLIP-ZS	78.8 _{+2.3}	78.2 _{+3.2}	46.8 _{+2.3}	82.6 _{+3.3}	84.0 _{+0.1}	91.8 _{+1.2}	95.8 _{+1.1}	97.9 _{+2.3}	97.4 _{+0.6}	70.3 _{+4.2}	87.7 _{+3.8}	82.8 _{+2.2}
4-shot												
CoOp	78.2	77.5	55.4	87.2	89.1	89.8	94.6	99.1	97.2	74.1	87.2	84.5
+ TransCLIP-ZS	79.5 _{+1.3}	79.8 _{+2.3}	54.6 _{-0.7}	90.5 _{+3.4}	88.0 _{-1.1}	91.5 _{+1.7}	95.4 _{+0.8}	99.4 _{+0.4}	98.1 _{+0.9}	75.3 _{+1.2}	89.0 _{+1.8}	85.6 _{+1.1}
TIP-Adapter-F	79.3	79.6	55.8	86.1	88.1	91.6	94.6	98.3	97.5	74.0	87.4	84.7
+ TransCLIP-ZS	80.1 _{+0.9}	80.0 _{+0.4}	56.0 _{+0.2}	88.8 _{+2.7}	87.4 _{-0.7}	91.9 _{+0.4}	95.7 _{+1.1}	99.1 _{+0.9}	97.9 _{+0.4}	73.9 _{-0.1}	88.8 _{+1.4}	85.4 _{+0.7}
TaskRes	78.1	76.7	55.0	83.7	87.6	91.5	94.6	97.7	97.2	74.2	86.2	83.9
+ TransCLIP-ZS	79.8 _{+1.7}	79.4 _{+2.7}	52.9 _{-2.2}	85.3 _{+1.6}	85.4 _{-2.2}	92.0 _{+0.5}	95.3 _{-0.7}	99.4 _{+1.7}	97.8 _{+0.6}	72.6 ₋		

Table 14: Cross-Dataset transferability evaluation for five encoders. Few-shot learning methods are trained on 16-shot ImageNet and evaluate on the ten other fine-grained datasets. Average excludes ImageNet.

Method	Source	Target										Average	
	ImageNet	SUN397	Aircraft	EuroSAT	StanfordCars	Food101	Pets	Flower102	Caltech101	DTD	UCF101		
ResNet-50	CoOp	63.0	56.5	13.8	22.7	53.1	73.6	84.2	56.7	85.7	34.5	56.9	53.8
	+ TransCLIP-ZS	63.5 _{+0.5}	62.4 _{+5.9}	14.2 _{+0.4}	38.6 _{+16.0}	56.1 _{+3.0}	76.2 _{+2.6}	84.7 _{+0.5}	66.2 _{+9.5}	87.4 _{+1.7}	38.3 _{+3.7}	62.5 _{+5.6}	58.7 _{+4.9}
	CoCoOp	63.2	61.5	16.5	27.1	55.9	78.1	88.2	65.5	88.6	39.6	61.1	58.2
	+ TransCLIP-ZS	66.5 _{+3.2}	63.2 _{+1.7}	16.5 _{0.1}	36.0 _{+8.9}	57.2 _{+1.3}	74.7 _{-3.5}	86.1 _{-2.1}	70.8 _{+5.3}	88.5 _{0.1}	43.3 _{+3.7}	65.0 _{+3.9}	60.1 _{+1.9}
ResNet-101	CoOp	63.4	58.4	13.5	24.2	52.6	75.9	85.9	61.8	85.9	36.1	57.6	55.2
	+ TransCLIP-ZS	63.5 _{+0.2}	63.3 _{+4.9}	14.1 _{+0.6}	37.2 _{+13.0}	55.7 _{+3.0}	77.2 _{+1.3}	87.5 _{+1.6}	70.0 _{+8.2}	88.5 _{+2.6}	42.1 _{+6.0}	62.5 _{+4.9}	59.8 _{+4.6}
	CoCoOp	65.2	62.9	17.8	25.8	62.8	81.4	87.2	64.0	91.3	39.8	61.1	59.4
	+ TransCLIP-ZS	73.4 _{+8.1}	65.6 _{+2.7}	17.8 _{0.1}	45.2 _{+19.3}	67.3 _{+4.4}	79.9 _{-1.5}	87.1 _{-0.1}	71.6 _{+7.6}	90.9 _{0.4}	40.0 _{+0.3}	67.4 _{+6.3}	63.3 _{+3.9}
ViT-B/32	CoOp	66.8	60.6	14.2	31.8	56.9	78.8	85.6	58.9	90.3	35.9	61.8	57.5
	+ TransCLIP-ZS	68.4 _{+1.6}	65.7 _{+5.0}	14.9 _{+0.7}	49.5 _{+17.7}	60.4 _{+3.5}	80.4 _{+1.5}	86.5 _{+0.9}	68.0 _{+9.0}	92.9 _{+2.6}	40.4 _{+4.5}	67.6 _{+5.8}	62.6 _{+5.1}
	CoCoOp	66.0	64.6	17.8	40.5	59.6	80.8	88.2	65.4	92.1	42.7	64.9	61.7
	+ TransCLIP-ZS	71.9 _{+5.9}	67.4 _{+2.8}	17.8 _{+0.0}	54.4 _{+13.9}	61.0 _{+1.5}	79.0 _{-1.9}	85.7 _{-2.5}	73.9 _{+8.5}	92.4 _{+0.3}	47.8 _{+5.1}	71.0 _{+6.0}	65.0 _{+3.4}
ViT-L/14	ProGrad	66.9	61.9	13.5	33.4	56.3	79.6	86.3	60.8	91.4	38.0	62.5	58.4
	+ TransCLIP-ZS	68.4 _{+1.5}	66.3 _{+4.5}	14.2 _{+0.7}	51.7 _{+18.4}	59.8 _{+3.5}	80.8 _{+1.3}	86.9 _{+0.6}	70.9 _{+10.1}	92.5 _{+1.0}	42.5 _{+4.5}	67.8 _{+5.3}	63.4 _{+5.0}
	MaPLE	65.7	65.0	18.1	41.0	60.6	80.8	88.4	65.5	91.6	42.3	63.6	61.7
	+ TransCLIP-ZS	71.4 _{+5.8}	67.7 _{+2.7}	18.5 _{+0.4}	54.6 _{+13.6}	60.4 _{-0.2}	78.7 _{-2.2}	85.4 _{-3.0}	72.5 _{+7.0}	92.2 _{+0.6}	46.8 _{+4.5}	68.8 _{+5.3}	64.6 _{+2.9}
ViT-B/16	MaPLE w/ PromptAlign	/	66.1	18.8	39.7	63.5	82.1	88.4	66.1	92.1	42.5	65.6	62.5
	CoOp	71.9	62.0	15.7	44.6	62.1	84.3	88.3	67.1	92.7	39.5	64.1	62.0
	+ TransCLIP-ZS	73.3 _{+1.4}	67.4 _{+5.4}	17.1 _{+1.4}	54.5 _{+9.9}	66.8 _{+4.8}	86.3 _{+2.0}	89.4 _{+1.1}	74.2 _{+7.2}	93.4 _{+0.7}	42.1 _{+2.6}	69.9 _{+5.7}	66.1 _{+4.1}
	CoCoOp	71.1	67.0	22.7	44.6	64.9	86.2	90.7	71.6	93.9	45.2	68.8	65.6
ViT-L/16	+ TransCLIP-ZS	76.8 _{+5.7}	69.6 _{+2.7}	22.6 _{0.1}	59.2 _{+14.6}	67.0 _{-2.1}	85.4 _{-0.8}	89.8 _{-0.9}	79.0 _{+7.4}	94.3 _{-0.3}	50.6 _{+5.4}	74.5 _{-5.7}	69.2 _{+3.6}
	ProGrad	72.1	63.9	21.6	38.9	64.0	85.9	90.2	67.8	92.9	43.2	65.9	63.4
	+ TransCLIP-ZS	73.5 _{+1.4}	68.6 _{+4.7}	22.7 _{+1.1}	55.2 _{+16.4}	67.9 _{+3.8}	87.0 _{+1.2}	91.3 _{+1.1}	73.9 _{-6.1}	94.0 _{+1.1}	46.6 _{+3.4}	73.5 _{+7.6}	68.1 _{+4.6}
	PromptSRC	71.4	67.3	24.1	45.0	65.6	86.5	90.1	70.5	93.8	46.2	68.9	65.8
ViT-L/14	+ TransCLIP-ZS	76.9 _{+5.5}	69.9 _{+2.6}	24.9 _{+0.8}	59.4 _{+14.4}	67.6 _{+2.0}	85.3 _{-1.2}	89.4 _{-0.7}	76.7 _{+6.2}	94.2 _{+0.4}	51.1 _{+5.0}	76.0 _{+7.0}	69.4 _{+3.7}
	MaPLE	70.5	67.3	24.4	45.8	65.7	86.4	90.4	72.0	93.7	46.3	68.7	66.2
	+ TransCLIP-ZS	76.6 _{+6.1}	69.8 _{+2.5}	24.5 _{+0.2}	59.5 _{+13.7}	66.8 _{+1.2}	85.4 _{-1.0}	89.7 _{-0.7}	78.0 _{+6.0}	94.3 _{+0.6}	49.4 _{+3.1}	74.4 _{+5.6}	69.1 _{+3.1}
	MaPLE w/ PromptAlign	/	67.5	24.8	47.9	68.5	86.7	90.8	72.4	94.0	47.2	69.5	66.9
ViT-B/16	CoOp	78.2	64.9	21.6	51.4	75.5	89.3	91.0	68.9	93.6	43.6	68.8	66.9
	+ TransCLIP-ZS	79.5 _{+1.4}	70.6 _{+5.7}	24.3 _{+2.8}	72.7 _{+21.3}	79.0 _{+3.4}	91.1 _{+1.8}	93.6 _{+2.6}	78.1 _{+9.2}	96.2 _{+2.5}	48.2 _{+4.6}	75.3 _{+6.5}	72.9 _{+6.0}
	CoCoOp	77.8	70.8	31.0	47.4	77.9	91.4	94.1	76.2	94.1	50.7	74.1	71.1
	+ TransCLIP-ZS	81.9 _{+4.1}	73.8 _{+3.0}	33.2 _{+2.1}	76.3 _{+28.9}	78.7 _{+0.8}	90.6 _{-0.8}	94.4 _{+0.3}	81.4 _{+5.1}	97.1 _{-0.1}	55.5 _{+4.7}	79.2 _{-5.1}	76.0 _{+4.9}
ViT-L/14	ProGrad	78.4	66.9	24.8	45.4	75.9	90.4	93.1	73.4	95.3	45.8	71.8	68.3
	+ TransCLIP-ZS	79.6 _{+1.2}	72.4 _{+5.5}	26.8 _{+2.0}	67.2 _{+21.7}	78.7 _{+2.8}	91.6 _{+1.2}	95.6 _{+2.5}	79.4 _{-6.0}	96.6 _{+1.3}	51.9 _{+6.0}	78.4 _{+6.6}	73.8 _{+5.6}
	MaPLE	77.2	71.6	30.2	55.7	77.3	91.3	93.1	76.7	96.2	53.8	74.9	72.1
	+ TransCLIP-ZS	81.6 _{+4.4}	74.1 _{+2.5}	32.8 _{+2.6}	75.2 _{+19.6}	78.3 _{+1.0}	90.5 _{-0.8}	94.2 _{+1.1}	83.0 _{-6.3}	97.4 _{+1.2}	56.2 _{+2.4}	81.0 _{+6.1}	76.3 _{+4.2}

Table 15: Domain Generalization evaluation for five encoders with manual prompting strategies.

Method	Source	Target						
	ImageNet	Adversarial	ImageNetV2	Rendition	Sketch	Average	Average OOD	
ResNet-50	w/ a photo of a	58.0	22.0	51.2	56.1	33.3	44.1	40.7
	+ TransCLIP-ZS	60.8 _{+2.8}	21.5 _{-0.4}	51.4 _{+0.1}	52.8 _{-3.3}	35.1 _{+1.8}	44.3 _{+0.2}	40.2 _{-0.5}
	w/ custom templates	60.3	23.8	53.4	60.5	35.5	46.7	43.3
	+ TransCLIP-ZS	61.7 _{+1.4}	23.4 _{-0.5}	52.6 _{-0.8}	56.4 _{-4.2}	36.6 _{+1.1}	46.1 _{-0.6}	42.2 _{-1.1}
ResNet-101	w/ a photo of a	60.6	28.2	54.3	64.2	38.0	49.1	46.2
	+ TransCLIP-ZS	64.8 _{+4.2}	29.2 _{+1.0}	56.2 _{+1.9}	65.1 _{+1.0}	42.2 _{+4.3}	51.5 _{+2.5}	48.2 _{+2.0}
	w/ custom templates	62.5	29.8	56.1	67.7	40.6	51.4	48.6
	+ TransCLIP-ZS	65.6 _{+3.0}	30.6 _{+0.8}	57.0 _{+0.9}	68.2 _{+0.5}	44.0 _{+3.4}	53.1 _{+1.7}	49.9 _{+1.4}
ViT-B/32	w/ a photo of a	61.9	29.9	54.7	66.8	40.8	50.8	48.1
	+ TransCLIP-ZS	64.9 _{+3.0}	30.5 _{+0.6}	55.7 _{+1.1}	67.0 _{+0.2}	43.6 _{+2.8}	52.4 _{+1.5}	49.2 _{+1.2}
	w/ custom templates	63.8	32.1	56.3	69.5	42.1	52.8	50.0
	+ TransCLIP-ZS	66.2 _{+2.5}	32.4 _{+0.3}	56.6 _{+0.2}	69.2 _{-0.3}	44.3 _{+2.1}	53.7 _{+1.0}	50.6 _{+0.6}
ViT-B/16	w/ a photo of a	66.6	47.9	60.6	73.8	46.0	59.0	57.1
	+ TransCLIP-ZS	70.3 _{+3.7}	49.5 _{+1.7}	62.3 _{+1.7}	75.0 _{+1.3}	49.7 _{+3.7}	61.4 _{+2.4}	59.1 _{+2.1}
	w/ custom templates	68.8	50.6	62.3	77.8	48.4	61.6	59.8
	+ TransCLIP-ZS	71.5 _{+2.7}	52.1 _{+1.4}	63.4 _{+1.1}	78.1 _{+0.2}	51.1 _{+2.7}	63.2 _{+1.6}	61.2 _{+1.4}
ViT-L/14	w/ a photo of a	72.9	68.4	67.2	85.3	57.4	70.2	69.6
	+ TransCLIP-ZS	77.2 _{+4.3}	71.4 _{+3.0}	69.1 _{+1.8}	87.1 _{+1.8}	60.0 _{+2.6}	72.9 _{+2.7}	71.9 _{+2.3}
	w/ custom templates	75.9	70.9	70.2	87.8	59.7	72.9	72.2
	+ TransCLIP-ZS	78.6 _{+2.7}	73.6 _{+2.7}	70.8 _{+0.5}	89.0 _{+1.1}	61.9 _{+2.2}	74.8 _{+1.8}	73.8 _{+1.6}

Table 16: Domain Generalization evaluation for five encoders. Few-shot learning methods are trained on 16-shot ImageNet and evaluated on the 4 other variants.

Method	Source		Target				Average	Average OOD
	ImageNet	Adversarial	ImageNetV2	Rendition	Sketch			
ResNet-50	CoOp	63.0	22.0	55.0	55.0	32.8	45.5	41.2
	+ TransCLIP-ZS	63.5 _{+0.5}	21.0 _{-1.0}	53.6 _{-1.4}	52.3 _{-2.7}	34.8 _{+2.0}	45.0 _{-0.5}	40.4 _{-0.8}
	TaskRes	64.6	22.9	56.4	60.8	35.9	48.1	44.0
	+ TransCLIP-ZS	64.4 _{-0.2}	21.7 _{-1.2}	54.8 _{-1.6}	56.2 _{-4.6}	36.9 _{+1.0}	46.8 _{-1.3}	42.4 _{+1.6}
ResNet-101	CoOp	66.5	29.5	58.3	63.6	39.0	51.4	47.6
	+ TransCLIP-ZS	68.5 _{+2.0}	29.9 _{+0.5}	58.6 _{+0.2}	64.8 _{+1.2}	42.3 _{+3.3}	52.8 _{+1.4}	48.9 _{+1.3}
	TaskRes	67.6	30.0	59.6	68.4	41.8	53.5	49.9
	+ TransCLIP-ZS	69.3 _{+1.7}	30.2 _{+0.2}	59.3 _{-0.4}	68.8 _{+0.4}	44.6 _{+2.9}	54.4 _{+1.0}	50.7 _{+0.8}
ViT-B/32	CoOp	66.8	31.2	58.5	65.2	40.1	52.3	48.7
	+ TransCLIP-ZS	68.4 _{+1.6}	31.3 _{+0.1}	58.3 _{-0.2}	65.5 _{+0.3}	42.7 _{+2.6}	53.2 _{+0.9}	49.4 _{+0.7}
	TaskRes	68.2	31.3	59.3	69.5	42.5	54.2	50.6
	+ TransCLIP-ZS	69.2 _{+1.1}	31.3 _{+0.1}	59.1 _{-0.2}	69.3 _{-0.3}	44.9 _{+2.4}	54.8 _{+0.6}	51.2 _{+0.5}
ViT-B/16	CoOp	71.9	49.4	64.1	75.1	47.1	61.5	58.9
	+ TransCLIP-ZS	73.3 _{+1.4}	50.8 _{+1.3}	64.6 _{+0.4}	75.7 _{+0.7}	50.3 _{+3.2}	62.9 _{+1.4}	60.4 _{+1.4}
	TaskRes	73.0	50.3	65.6	77.8	49.2	63.2	60.7
	+ TransCLIP-ZS	74.1 _{+1.0}	51.9 _{+1.6}	65.4 _{-0.2}	78.4 _{+0.6}	51.6 _{+2.4}	64.3 _{+1.1}	61.8 _{+1.1}
ViT-L/14	CoOp	78.2	69.4	70.8	85.4	57.5	72.3	70.8
	+ TransCLIP-ZS	79.5 _{+1.3}	71.9 _{+2.6}	71.1 _{+0.3}	86.9 _{+1.5}	60.0 _{+2.5}	73.9 _{+1.6}	72.5 _{+1.7}
	TaskRes	78.1	71.3	71.6	87.9	60.1	73.8	72.7
	+ TransCLIP-ZS	79.8 _{+1.7}	74.2 _{+3.0}	71.8 _{+0.2}	88.9 _{+1.1}	62.0 _{+1.9}	75.4 _{+1.6}	74.2 _{+1.5}

Table 17: Detailed results of transductive methods in the few-shot setting for the 11 datasets with ResNet-50 as visual backbone.

Shots	Method	ImageNet	SUN	Aircraft	EuroSAT	Cars	Food	Pets	Flowers	Caltech	DTD	UCF	Average
1	TF	20.6	31.2	13.1	39.0	21.8	28.3	27.2	53.6	66.1	27.7	38.1	33.3
	BD-CSPN	24.7	36.9	13.9	40.3	27.2	34.1	34.1	66.7	74.3	32.8	43.4	38.9
	LaplacianShot	23.8	35.5	14.0	42.3	27.0	34.7	37.3	66.6	72.4	32.8	43.2	39.1
	PT-MAP	29.4	42.9	15.7	48.0	33.8	44.8	56.5	61.4	46.9	38.6	52.2	42.7
	TIM	26.1	40.0	13.4	42.5	27.3	41.4	35.0	69.1	62.3	31.7	46.9	39.6
	CoOp + UPL	59.6	63.4	17.5	54.7	56.4	75.3	82.8	73.5	87.4	48.3	66.1	62.3
	TransCLIP-FS	55.7	63.5	20.6	70.3	56.2	77.2	86.9	83.7	87.4	51.3	70.7	65.8
	TF	29.6	43.1	16.6	57.2	32.3	41.4	40.1	68.4	77.5	41.4	51.3	45.4
2	BD-CSPN	33.2	48.1	17.8	58.6	36.2	47.4	50.0	77.0	80.7	43.2	54.1	49.7
	LaplacianShot	33.1	47.8	17.7	60.0	36.1	48.7	50.4	77.5	81.0	43.3	55.2	50.1
	PT-MAP	39.3	54.6	19.3	61.4	43.5	60.1	67.0	68.9	51.5	50.4	61.9	52.5
	TIM	35.5	52.2	18.2	60.2	38.1	57.2	51.7	79.7	76.1	44.2	59.6	52.1
	CoOp + UPL	59.8	64.0	19.3	62.9	59.2	74.8	81.2	80.5	88.1	49.5	68.0	64.3
	TransCLIP-FS	59.3	66.2	20.3	71.5	58.7	77.2	86.0	87.1	87.8	55.2	72.8	67.5
	TF	38.5	53.1	20.4	64.9	42.8	52.5	49.3	80.7	83.6	48.4	59.3	54.0
	4	BD-CSPN	40.7	54.9	20.2	65.4	43.4	56.6	54.3	83.7	84.0	48.1	59.8
LaplacianShot		40.5	54.9	19.7	68.0	43.3	58.0	55.5	84.2	83.9	47.9	60.1	56.0
PT-MAP		46.8	61.4	22.8	69.5	50.7	66.6	70.0	71.0	54.6	56.3	68.0	58.0
TIM		43.3	59.1	22.9	71.0	49.6	64.0	58.8	87.6	79.1	53.2	65.8	59.5
CoOp + UPL		60.3	65.7	23.3	71.0	63.0	75.8	83.6	87.3	88.0	55.2	69.1	67.5
TransCLIP-FS		59.3	66.5	25.0	73.8	61.4	76.6	81.6	88.4	88.2	57.6	73.3	68.4
TF		45.1	59.7	24.1	66.8	51.2	61.1	61.7	86.4	86.3	55.9	65.1	60.3
8		BD-CSPN	45.6	59.6	22.9	66.2	50.4	62.4	65.7	87.5	85.5	54.6	65.1
	LaplacianShot	45.2	59.1	22.4	69.1	49.6	63.4	65.7	87.6	85.8	53.9	65.9	60.7
	PT-MAP	50.6	64.2	23.4	66.7	55.9	69.6	76.9	72.9	54.8	60.4	70.6	60.5
	TIM	49.9	63.4	25.0	69.5	59.7	70.0	71.8	89.9	82.9	59.1	70.8	64.7
	CoOp + UPL	60.9	67.0	26.0	71.7	66.5	75.5	82.7	91.2	88.3	59.0	71.4	69.1
	TransCLIP-FS	59.9	68.3	28.0	74.5	67.6	76.9	86.6	90.4	88.7	62.1	76.1	70.8
	TF	50.0	63.2	26.6	71.8	57.7	66.1	66.4	90.3	87.3	58.8	67.7	64.2
	16	BD-CSPN	49.7	62.4	25.5	71.3	56.6	66.0	66.2	89.6	86.7	57.8	67.2
LaplacianShot		48.9	61.5	24.6	71.5	54.8	66.7	67.5	89.5	86.4	56.2	67.5	63.2
PT-MAP		54.1	66.1	25.6	68.1	61.1	70.6	79.0	75.2	57.0	62.4	71.0	62.7
TIM		55.5	66.8	30.8	81.6	68.0	72.4	75.0	88.9	85.7	63.1	74.4	69.3
CoOp + UPL		60.9	69.4	31.6	78.0	71.4	76.2	83.5	93.6	89.1	62.8	73.5	71.8
TransCLIP-FS		62.6	70.4	30.3	77.6	71.5	77.1	87.3	92.5	88.7	64.4	77.7	72.7

Table 18: Detailed results of transductive methods in the few-shot setting for the 11 datasets with ResNet-101 as visual backbone.

Shots	Method	ImageNet	SUN	Aircraft	EuroSAT	Cars	Food	Pets	Flowers	Caltech	DTD	UCF	Average
1	TF	24.9	33.3	16.0	38.5	29.4	34.3	37.1	57.0	71.6	29.7	43.5	37.8
	BD-CSPN	29.9	40.2	16.8	39.5	35.1	42.6	51.0	70.0	79.6	32.1	51.8	44.4
	LaplacianShot	30.0	40.0	17.1	40.6	37.2	43.8	51.8	71.7	79.4	34.9	52.1	45.3
	PT-MAP	34.3	46.2	18.1	49.3	44.0	53.0	69.5	65.0	51.6	39.1	58.9	48.1
	TIM	31.5	44.2	16.6	42.9	39.0	54.9	51.8	77.6	66.5	36.1	56.2	47.0
	CoOp + UPL	62.7	64.5	20.8	63.6	61.7	77.8	83.8	72.8	89.6	47.0	69.1	64.9
	TransCLIP-FS	64.3	66.6	19.6	67.2	70.0	82.9	91.5	80.4	91.2	47.0	70.1	68.3
2	TF	34.8	46.6	19.6	53.7	41.2	49.1	51.1	73.8	83.1	42.3	56.3	50.1
	BD-CSPN	39.9	51.7	20.3	54.2	46.7	57.7	60.4	80.8	85.5	45.5	59.4	54.7
	LaplacianShot	39.9	51.8	20.9	59.3	46.9	59.0	63.2	81.9	85.9	45.5	59.8	55.8
	PT-MAP	44.3	57.4	21.8	62.0	52.9	65.7	76.6	71.0	56.2	52.5	65.8	56.9
	TIM	42.4	55.6	19.9	63.5	50.2	69.2	67.3	85.5	81.5	49.0	62.6	58.8
	CoOp + UPL	63.0	65.4	23.6	66.4	66.6	77.8	85.2	81.2	89.4	51.4	70.9	67.4
	TransCLIP-FS	64.6	67.2	22.7	68.3	70.7	80.8	89.1	85.2	91.5	49.8	72.8	69.3
4	TF	44.9	56.9	23.7	62.8	53.4	61.6	61.1	83.7	87.5	51.5	65.4	59.3
	BD-CSPN	47.8	58.8	23.7	62.1	54.4	66.0	70.1	86.1	87.7	51.2	65.4	61.2
	LaplacianShot	47.7	58.9	23.4	71.9	54.3	67.3	70.9	86.8	87.7	51.1	65.8	62.3
	PT-MAP	51.7	63.8	25.5	68.0	60.3	71.6	79.9	74.6	56.4	57.4	71.0	61.8
	TIM	51.2	63.2	25.1	73.6	61.4	75.8	76.8	87.0	87.8	55.3	71.7	66.3
	CoOp + UPL	63.9	67.4	25.4	70.8	69.3	79.5	85.5	87.4	90.3	55.6	73.2	69.2
	TransCLIP-FS	65.1	68.7	26.2	73.7	71.6	81.3	90.1	88.6	91.7	56.4	73.2	71.5
8	TF	51.5	62.9	27.1	63.3	61.5	69.0	72.3	89.1	89.7	58.2	70.2	65.0
	BD-CSPN	52.7	63.1	27.3	62.7	61.0	70.9	76.8	89.5	89.4	57.0	70.3	65.5
	LaplacianShot	52.3	62.8	26.8	68.4	60.7	71.7	77.3	89.6	89.2	56.0	70.3	65.9
	PT-MAP	55.5	66.5	28.1	67.0	64.6	73.7	84.6	76.6	59.4	61.1	72.2	64.5
	TIM	56.6	67.3	28.1	74.3	70.0	77.0	85.3	91.5	88.6	60.5	71.7	70.1
	CoOp + UPL	64.6	69.0	28.3	77.9	73.5	79.5	85.8	92.1	90.7	61.2	75.8	72.6
	TransCLIP-FS	65.0	69.6	27.9	71.2	74.4	81.5	90.3	89.0	91.7	61.7	76.1	72.6
16	TF	56.3	66.8	30.7	68.0	68.0	73.6	76.3	92.0	90.9	61.9	72.6	68.8
	BD-CSPN	56.4	66.1	30.8	66.0	67.2	73.4	76.4	91.8	90.8	60.5	72.4	68.3
	LaplacianShot	56.0	65.5	29.4	71.2	65.8	74.4	78.6	91.7	90.2	58.8	72.3	68.5
	PT-MAP	58.6	68.3	30.9	69.5	69.2	75.3	85.3	78.2	61.5	62.9	73.4	66.6
	TIM	61.4	70.6	34.6	79.2	75.8	78.8	84.4	91.8	88.9	67.2	76.4	73.6
	CoOp + UPL	64.6	71.1	34.9	82.1	77.6	79.5	85.7	94.0	92.1	65.2	77.1	74.9
	TransCLIP-FS	66.4	71.1	28.4	73.8	77.1	81.6	90.6	90.8	92.3	61.5	76.8	73.7

Table 19: Detailed results of transductive methods in the few-shot setting for the 11 datasets with ViT-B/32 as visual backbone.

Shots	Method	ImageNet	SUN	Aircraft	EuroSAT	Cars	Food	Pets	Flowers	Caltech	DTD	UCF	Average
1	TF	25.1	36.1	14.6	44.4	26.7	34.4	33.3	60.0	74.4	29.0	46.4	38.6
	BD-CSPN	30.1	42.9	16.2	45.7	33.8	41.2	43.9	73.1	80.2	30.8	52.6	44.6
	LaplacianShot	29.2	41.7	16.1	48.6	33.2	43.1	43.8	73.3	80.6	32.7	52.9	45.0
	PT-MAP	33.1	48.8	17.0	54.8	38.6	49.8	50.9	62.4	52.5	37.9	57.0	45.7
	TIM	31.5	47.6	16.6	55.2	36.4	51.4	48.4	76.8	71.5	35.6	57.6	48.1
	CoOp + UPL	63.0	66.2	21.0	64.0	58.1	78.8	84.0	74.4	89.7	52.0	68.3	65.4
	TransCLIP-FS	64.3	68.9	22.7	63.5	63.7	82.2	90.1	83.2	92.2	52.3	69.5	68.4
2	TF	34.7	49.5	19.3	56.5	37.4	48.7	47.4	75.1	83.9	44.5	57.7	50.4
	BD-CSPN	39.2	53.1	20.7	57.2	42.1	55.5	55.2	82.4	86.8	45.6	61.6	54.5
	LaplacianShot	39.1	53.9	20.4	58.3	42.4	57.7	57.3	82.5	86.7	45.9	62.6	55.2
	PT-MAP	42.6	60.1	22.3	63.7	46.0	63.9	64.0	69.5	55.6	50.4	66.8	55.0
	TIM	41.1	59.0	21.1	68.9	44.1	66.2	60.1	86.5	81.5	48.6	68.1	58.7
	CoOp + UPL	63.4	66.6	22.8	71.9	60.8	78.5	85.0	81.0	90.1	53.5	70.2	67.6
	TransCLIP-FS	64.8	69.5	22.9	76.9	63.8	81.2	89.9	85.4	92.1	52.9	71.0	70.0
4	TF	44.5	59.4	23.2	62.1	48.6	60.8	57.9	85.2	89.1	52.6	65.2	59.0
	BD-CSPN	47.0	61.1	23.4	64.2	49.1	65.3	64.8	87.2	89.4	52.0	67.0	61.0
	LaplacianShot	46.8	61.1	23.6	68.4	49.2	65.6	66.6	87.6	89.3	51.4	67.5	61.6
	PT-MAP	50.1	65.5	24.1	68.9	52.3	70.3	69.0	73.3	57.3	56.1	70.1	59.7
	TIM	50.4	65.0	24.7	70.0	56.1	73.0	74.4	90.5	88.7	55.9	71.8	65.5
	CoOp + UPL	63.9	68.8	26.6	72.6	63.7	78.2	85.2	88.8	90.1	55.4	73.1	69.7
	TransCLIP-FS	64.7	70.1	26.4	78.0	66.5	80.3	87.2	88.7	92.2	58.0	74.3	71.5
8	TF	50.9	64.7	27.1	67.6	57.1	68.5	68.0	89.4	90.5	58.2	70.7	64.8
	BD-CSPN	51.2	64.8	27.4	66.5	56.9	69.6	71.7	90.0	89.6	56.3	71.0	65.0
	LaplacianShot	51.0	64.3	26.4	70.0	55.9	70.4	73.7	90.2	90.1	55.4	70.8	65.3
	PT-MAP	53.7	68.3	27.4	70.9	58.5	72.8	75.4	75.2	59.7	59.4	71.5	63.0
	TIM	56.2	69.0	28.4	75.8	65.1	76.1	79.6	92.3	87.4	63.3	75.4	69.9
	CoOp + UPL	64.8	69.7	30.0	79.6	68.9	79.3	85.5	91.6	91.8	62.1	73.9	72.5
	TransCLIP-FS	65.5	71.3	28.0	78.2	70.8	81.0	89.4	90.0	92.3	61.1	77.0	73.2
16	TF	55.6	68.0	29.7	69.7	62.9	72.6	73.7	92.0	91.6	61.6	73.1	68.2
	BD-CSPN	55.3	67.5	29.8	69.5	62.3	72.9	74.2	91.9	91.7	59.6	73.3	68.0
	LaplacianShot	54.8	66.7	28.4	71.2	60.9	73.2	75.3	91.3	91.3	58.3	72.9	67.7
	PT-MAP	56.9	69.9	29.2	71.3	63.1	74.1	78.7	77.1	60.7	61.9	72.9	65.1
	TIM	60.5	71.8	33.0	79.4	72.2	78.1	85.0	92.8	88.4	66.6	78.1	73.3
	CoOp + UPL	64.8	71.9	34.1	84.3	73.6	79.0	85.8	94.2	92.4	64.8	78.3	74.8
	TransCLIP-FS	66.6	72.6	30.1	78.9	73.2	81.1	89.5	90.9	94.4	62.7	77.2	74.3

Table 20: Detailed results of transductive methods in the few-shot setting for the 11 datasets with ViT-B/16 as visual backbone.

Shots	Method	ImageNet	SUN	Aircraft	EuroSAT	Cars	Food	Pets	Flowers	Caltech	DTD	UCF	Average
1	TF	29.7	38.1	19.2	46.0	32.5	43.5	38.2	67.8	75.5	31.6	48.8	42.8
	BD-CSPN	35.4	45.7	22.0	45.7	42.0	54.2	52.9	82.9	83.5	34.7	58.0	50.6
	LaplacianShot	34.9	44.5	22.1	52.1	41.1	53.0	52.2	83.1	83.4	35.8	57.3	50.9
	PT-MAP	40.1	52.6	23.8	59.7	48.4	64.4	61.8	69.4	54.1	41.8	63.5	52.7
	TIM	37.5	48.3	22.8	48.2	44.8	65.7	53.9	86.4	75.1	35.8	62.7	52.8
	CoOp + UPL	68.8	68.5	27.2	70.0	68.9	83.6	90.6	81.7	92.7	51.3	73.1	70.6
	TransCLIP-FS	69.8	70.6	29.9	72.5	70.9	87.9	93.8	84.8	93.1	53.3	78.4	73.2
	TF	40.5	51.6	25.3	63.1	45.1	58.8	54.8	83.2	87.0	47.3	59.4	56.0
2	BD-CSPN	46.1	56.1	26.7	64.7	50.7	67.5	64.6	89.6	89.6	48.9	64.0	60.8
	LaplacianShot	45.8	55.9	27.1	68.2	51.1	68.2	66.0	89.7	89.6	48.9	65.1	61.4
	PT-MAP	50.7	63.1	28.6	71.7	57.5	77.5	75.7	73.9	59.1	53.8	68.7	61.9
	TIM	47.9	60.7	28.1	75.8	55.7	78.7	70.6	91.4	86.6	52.3	66.4	64.9
	CoOp + UPL	69.2	69.2	30.1	73.4	71.0	83.8	88.4	87.9	93.3	53.9	75.8	72.4
	TransCLIP-FS	70.3	70.9	30.0	77.1	71.7	87.0	91.7	90.6	93.5	55.1	78.5	74.2
	TF	51.1	61.0	30.3	64.9	56.8	71.0	65.9	90.9	91.5	53.7	67.9	64.1
	4	BD-CSPN	53.8	62.5	30.5	64.8	58.5	75.3	72.0	92.5	92.0	52.1	70.9
LaplacianShot		53.5	62.5	29.6	74.3	58.5	75.7	73.4	92.8	92.0	52.7	71.7	67.0
PT-MAP		57.6	68.1	31.2	74.9	63.1	81.1	79.5	76.2	60.2	58.4	73.9	65.8
TIM		57.4	67.0	32.8	79.3	65.8	83.5	82.3	93.4	88.5	58.1	76.5	71.3
CoOp + UPL		69.7	71.4	32.6	74.0	74.6	83.8	91.3	92.1	93.2	58.9	76.9	74.4
TransCLIP-FS		70.3	71.9	34.0	79.4	74.0	86.4	91.6	93.6	94.0	61.1	79.1	75.9
TF		57.2	66.8	34.7	68.5	65.4	77.4	74.3	93.8	92.4	60.3	73.8	69.5
8		BD-CSPN	57.9	66.5	34.1	68.3	64.6	78.0	77.2	93.2	92.4	59.0	74.2
	LaplacianShot	57.6	65.9	33.4	73.2	64.7	79.3	79.3	93.3	92.3	56.5	74.6	70.0
	PT-MAP	61.0	70.6	34.1	75.0	68.5	82.0	84.5	77.2	62.1	62.4	75.6	68.5
	TIM	62.6	71.3	35.9	79.8	74.4	84.3	87.4	94.0	90.7	63.6	80.2	74.9
	CoOp + UPL	70.5	72.8	38.6	79.1	78.3	84.5	90.4	94.4	93.3	60.6	79.6	76.6
	TransCLIP-FS	70.5	73.2	36.4	79.7	76.9	86.7	91.9	93.9	94.2	65.7	81.5	77.3
	TF	61.8	70.1	38.3	74.3	71.2	80.7	79.5	95.4	93.6	62.9	76.0	73.1
	16	BD-CSPN	61.7	69.4	37.7	73.4	70.7	80.2	81.2	94.8	93.3	61.3	76.0
LaplacianShot		60.9	68.3	36.1	78.1	69.2	81.2	81.7	94.8	93.1	58.6	76.3	72.6
PT-MAP		64.0	72.0	37.4	75.6	72.0	82.7	86.1	78.5	63.7	63.7	76.3	70.2
TIM		67.8	73.6	40.6	83.6	79.5	84.9	88.7	95.4	92.4	67.5	82.1	77.8
CoOp + UPL		71.6	75.1	43.2	83.0	82.3	85.0	90.4	95.8	94.3	68.7	80.4	79.1
TransCLIP-FS		71.8	74.7	38.6	83.0	79.8	86.9	92.4	94.4	94.0	65.1	82.1	78.4

Table 21: Detailed results of transductive methods in the few-shot setting for the 11 datasets with ViT-L/14 as visual backbone.

Shots	Method	ImageNet	SUN	Aircraft	EuroSAT	Cars	Food	Pets	Flowers	Caltech	DTD	UCF	Average
1	TF	36.6	41.2	26.3	49.8	45.2	53.9	45.8	81.8	79.7	35.8	58.3	50.4
	BD-CSPN	45.3	50.5	28.9	53.3	57.5	67.3	66.7	93.4	88.4	39.6	67.2	59.8
	LaplacianShot	43.5	48.4	30.9	56.6	56.1	69.3	65.8	93.3	87.9	40.1	66.2	59.8
	PT-MAP	49.8	58.1	33.1	65.6	60.6	80.1	78.1	75.2	58.5	45.7	69.7	61.3
	TIM	47.7	56.0	31.1	62.8	61.1	79.7	74.2	95.4	80.1	41.7	71.5	63.8
	CoOp + UPL	76.0	72.6	35.8	72.7	79.2	89.5	93.2	86.8	94.9	60.3	81.1	76.6
	TransCLIP-FS	75.9	74.5	37.9	77.4	78.8	92.2	95.4	95.9	95.6	61.3	83.3	78.9
	TF	50.1	56.6	33.5	71.7	58.3	71.6	65.7	93.0	90.5	49.8	69.4	64.6
2	BD-CSPN	57.0	61.2	35.6	72.6	65.1	79.9	77.2	95.7	92.8	52.3	74.7	69.5
	LaplacianShot	56.5	61.3	35.9	76.8	65.4	80.3	77.4	96.2	93.3	52.4	74.8	70.0
	PT-MAP	61.3	68.0	37.0	78.4	68.4	87.3	86.7	77.9	61.1	56.5	75.2	68.9
	TIM	59.7	67.6	35.4	82.2	69.3	87.4	85.5	95.1	91.4	53.2	78.6	73.2
	CoOp + UPL	76.1	73.4	39.9	72.3	81.4	90.3	92.5	94.0	94.7	62.0	82.2	78.1
	TransCLIP-FS	76.8	75.1	40.0	82.1	79.9	91.8	95.0	96.6	95.9	62.6	83.2	79.9
	TF	61.6	66.5	40.6	71.4	69.6	81.9	79.0	96.4	94.4	58.5	77.5	72.5
	4	BD-CSPN	64.3	67.8	40.6	71.4	72.2	84.7	82.8	96.7	95.2	56.9	79.6
LaplacianShot		63.8	67.6	40.0	78.9	72.0	85.4	85.7	97.3	95.2	56.7	79.6	74.7
PT-MAP		68.0	72.7	41.7	77.4	73.8	88.9	89.9	78.3	62.9	60.1	79.2	72.1
TIM		68.9	72.7	42.0	78.4	77.8	90.0	92.3	97.4	91.1	63.5	83.7	78.0
CoOp + UPL		76.5	75.1	44.1	79.3	83.1	90.1	92.6	95.2	95.3	65.8	83.9	80.1
TransCLIP-FS		76.9	76.2	45.9	81.5	81.2	91.4	94.3	98.2	96.1	66.8	84.9	81.2
TF		67.4	72.0	45.6	76.1	76.5	86.2	85.1	97.2	95.1	65.1	81.5	77.1
8		BD-CSPN	68.0	71.5	44.8	76.1	76.5	86.8	86.8	97.3	94.9	63.8	81.3
	LaplacianShot	67.3	70.4	43.6	78.2	75.9	87.3	88.3	97.0	94.9	61.2	80.8	76.8
	PT-MAP	70.7	74.6	44.1	78.4	77.1	89.2	91.3	79.5	64.5	65.1	79.7	74.0
	TIM	73.1	76.4	46.7	86.8	83.2	89.5	92.7	96.9	94.4	70.2	81.3	81.0
	CoOp + UPL	76.9	75.8	49.6	81.7	85.5	90.1	93.2	95.9	95.3	65.6	84.0	81.2
	TransCLIP-FS	77.2	77.3	50.0	82.6	84.1	91.6	94.5	98.5	97.0	70.7	86.0	82.7
	TF	71.1	74.9	50.1	78.6	81.5	88.1	88.6	98.5	96.1	67.3	83.0	79.8
	16	BD-CSPN	71.1	74.4	49.4	78.1	81.2	88.0	89.8	98.4	95.8	66.5	82.5
LaplacianShot		69.8	72.7	47.0	81.7	80.2	88.0	90.1	98.0	95.7	63.3	82.8	79.0
PT-MAP		72.9	75.9	48.1	79.1	79.9	89.4	92.0	80.5	66.0	65.6	80.5	75.4
TIM		76.4	78.7	52.5	89.4	86.5	91.0	92.0	98.2	94.5	73.2	84.8	83.4
CoOp + UPL		76.9	77.2	54.1	85.9	87.8	90.6	93.2	97.1	95.6	72.8	86.2	83.4
TransCLIP-FS		77.8	78.7	53.0	84.4	86.3	91.6	94.8	98.8	97.3	71.2	86.5	83.7

Table 22: UPL* top-1 accuracy on ImageNet for 8, 16 and 32 top-confidence pseudo-labels drawn from the test set.

Architecture	$N = 8$	$N = 16$	$N = 32$
ResNet-50	60.60	61.60	59.66
ViT-B/16	68.92	69.62	68.87

Table 23: Prompt templates for each dataset.

(a) Prompt templates used in the experiments unless otherwise specified.

Dataset	Prompt template
ImageNet	"a photo of a []."
SUN397	"a photo of a []."
Aircraft	"a photo of a [], a type of aircraft."
EuroSAT	"a centered satellite photo of []."
Cars	"a photo of a []."
Food101	"a photo of [], a type of food."
Pets	"a photo of [], a type of pet."
Flower102	"a photo of a [], a type of flower."
Caltech101	"a photo of a []."
DTD	"[] texture."
UCF101	"a photo of a person doing []."

(b) Custom prompt templates for ImageNet dataset [49].

"itap of a []."
"a bad photo of the []."
"a origami []."
"a photo of the large []."
"a [] in a video game."
"art of the []."
"a photo of the small []."